

Response to the reviewer's comments

“Impact of anthropogenic emissions on biogenic secondary organic aerosol: Observation in the Pearl River Delta, South China” by Yu-Qing Zhang et al.

In the following, the comments made by the referees appear in black, while our replies are in blue, and the revised texts in the manuscript are in red.

Reviewer #1

This manuscript presents the annual variations of SOA tracers from biogenic VOCs at nine sites in PRD region. The measured biogenic SOA tracers are found to be correlated with O_x and anthropogenic sulfate, indicating the impacts of anthropogenic emissions on biogenic SOA formation. This is an extensive study by analyzing 170 filters. Overall, the data analysis is solid and the manuscript is well-written. I recommend publication after major revisions.

We thank the reviewer for the helpful comments and suggestions for this manuscript. We respond to the reviewer point by point below and modified the manuscript according to the comments.

Major Comments

1. Recent studies¹⁻² demonstrated that C_5 -alkene triols and 3-methyltetrahydrofuran-3,4-diols are largely GC/EI-MS artifacts from the degradation of methyltetrol sulfates and dimers. The authors used figure 7 (ternary plots) to argue that these tracers are indeed formed from different pathways rather than thermal decomposition. However, I beg to differ. The lack of correlation between IEPOX-derived SOA tracers and be explained by that the three tracers in figure 7 arise from the thermal decomposition of different dimers/OS and the parent dimers/OS concentration varies with sites and season. To fully prove that the three tracers are not decomposition products, the authors need to sample authentic methyltetrol sulfate standard with GC-MS.

Reply: We agree that thermal degradation of methyltetrol sulfates and dimers could produce C_5 -alkene triols, 3-methyltetrahydrofuran-3,4-diols and 2-methyltetrols during the GC/MS analysis (Watanabe et al., 2018). Using a hydrophilic interaction liquid chromatography (HILIC) method developed by Jason

Surratt group, Cui et al (2018) estimated that 30.0%, 42.8%, and 14.7% of C₅-alkene triols measured by GC/MS were attributed to the potential thermal degradation of the 2-methyltetrol sulfates in the SOA from β -IEPOX, and the PM_{2.5} samples from Look Rock and Manaus sites, respectively. The fractions of 2-methyltetrols attributed to thermal degradation were 11.1%. And approximately all 3-MeTHF-3,4-diols were produced from thermal degradation. Recently, we also measured 2-methyltetrol sulfates in two samples at HS and TS sites, respectively (see Table R1-1 below). Assuming that all the 2-methyltetrol sulfates decomposed to these tracers, the thermal decomposition of 2-methyltetrol sulfates would account for 15.1-31.6% of C₅-alkene triols, 6.0-10.0% of 2-methyltetrols and all 3-methyltetrahydrofuran-3,4-diols measured by GC/MS. Thus, C₅-alkene triols and 2-methyltetrols are major from isoprene oxidation rather than thermal decomposition of 2-methyltetrol sulfates, while 3-methyltetrahydrofuran-3,4-diols are only in trace amount in the air and might be produced largely from thermal degradation. Coupled with significant variations in tracer compositions observed in the PRD, we believe that these SOA₁ tracers are mainly formed through different pathways in the ambient atmosphere, although part of them might arise from the thermal decomposition of different dimers/OSs and the parent dimers/OSs varies with sites and seasons.

All these discussion (see below) are added in the revised manuscript in line 250-271.

“Previous studies found that thermal decomposition of low volatility organics in IEPOX-derived SOA could produce SOA₁ tracers, e.g. 2-MTLs, C₅-alkene triols and 3-MeTHF-3,4-diols (Lopez-Hilfiker et al., 2016, Watanabe et al., 2018). This means that these tracers detected by GC-MSD might be generated from thermal decomposition of IEPOX-derived SOA. As estimated by Cui et al. (2018), 14.7-42.8% of C₅-alkene triols, 11.1% of 2-MTLs and approximately all 3-MeTHF-3,4-diols measured by GC/MSD could be attributed to the thermal degradation of 2-MTLs-derived organosulfates (MTL-OSs). We also measured MTL-OSs in two samples at HS and TS sites, respectively (Table S6) using the widely used LC-MS approach (He et al., 2014, 2018). Assuming that all MTL-OSs decomposed to these tracers, the thermal decomposition of MTL-OSs would account for 15.1-31.6% of C₅-alkene triols, 6.0-10.0% of 2-MTLs and all 3-MeTHF-3,4-diols measured by GC/MSD. Thus, C₅-alkene triols and 2-MTLs are major from isoprene oxidation rather than thermal decomposition of MTL-OSs, while 3-MeTHF-3,4-diols are only in trace amount in the air and might be produced largely from thermal degradation.

Moreover, we see significant variations in SOA₁ tracer compositions in the PRD. For instant, C₅-alkene triols have three isomers. If these tracers were mainly generated from a thermal process, their

compositions should be similar in different samples. In fact, the relative abundances of three C₅-alkene triol isomers significantly changed from site to site (Figure 7) and season to season (Figure S8), and their compositions in the PRD were different from those measured in the chamber samples (Lin et al., 2012). In addition, the slopes of linear correlations among these IEPOX-derived SOA tracers also varied from site to site (Figure S9). Coupled with the seasonal trend of 2-MGA/2-MTLs ratios, the apparent variations in SOA_I tracer compositions demonstrate that these SOA_I tracers are mainly formed through different pathways in the ambient atmosphere, although part of them might arise from the thermal decomposition of different dimers/OSs and the parent dimers/OSs varies with sites and seasons.”

Table R1-1 Concentrations of isoprene SOA products at HS and TS sites

	HS 20150701	TS 20150701
2-Methyltetrol sulfates (ng m ⁻³)	6.65	2.99
C ₅ -alkene triols (ng m ⁻³)	11.5	10.8
2-Methyltetrols (ng m ⁻³)	41.8	31.2
3-MeTHF-3,4-diols (ng m ⁻³)	0.482	0.227

Reference

1. Cui, T., Zeng, Z., dos Santos, E. O., Zhang, Z., Chen, Y., Zhang, Y., Rose, C. A., Budisulistiorini, S. H., Collins, L. B., Bodnar, W. M., de Souza, R. A. F., Martin, S. T., Machado, C. M. D., Turpin, B. J., Gold, A., Ault, A. P., and Surratt, J. D.: Development of a hydrophilic interaction liquid chromatography (HILIC) method for the chemical characterization of water-soluble isoprene epoxydiol (IEPOX)-derived secondary organic aerosol, *Environ. Sci.: Processes Impacts*, 20, 1524-1536, 10.1039/C8EM00308D, 2018.
2. Watanabe, A. C., Stropoli, S. J., and Elrod, M. J.: Assessing the potential mechanisms of isomerization reactions of isoprene epoxydiols on secondary organic aerosol, *Environ. Sci. Technol.*, 52, 8346-8354, 10.1021/acs.est.8b01780, 2018.

2. The authors use the BSOA vs sulfate slope to infer the magnitude of sulfate control on BSOA. As the authors have performed the same measurements in the same region for a long time, I encourage the authors to look at their historic measurements, based on which to estimate the sulfate-control magnitude. As shown in figure 1, the O₃ concentration has been relatively flat in the past 13 years, but SO₂ concentration has largely declined. This provides a nice opportunity to deconvolve the effect of sulfate vs O₃ on BSOA formation.

Reply: Thanks for the suggestion. Since 2007, we have carried out one-month campaign during fall-winter season every year at a regional site, Wanqingsha (WQS) in the PRD. At present, we have long-term data of sulfate from 2007 to 2016. Similar to SO₂, sulfate keeps decreasing in the past decade (see

Figure R1-1 below). Unfortunately, we have not completed the time-consuming measurements of BSOA tracers yet. Currently, we cannot deconvolve the effect of sulfate vs O_3 on BSOA formation based on long-term data. We will write another manuscript focusing on these long-term measurements and discussing the changing effects of sulfate and O_3 on BSOA formation.

Instead, we compared the data in 2015 with those during fall-winter season in 2008 at WQS (Ding et al., 2012), since BSOA tracers, sulfate and O_x were all measured in both studies. As the below Table R1-2 showed, all BSOA species positively correlated with sulfate but exhibited no O_x dependence. Thus, BSOA formation in 2008 was largely influenced by sulfate, probably due to high sulfate levels then (as high as $46.8 \mu\text{g m}^{-3}$). Coupled with the decrease trend of sulfate and the relatively flat trend of O_x , such a difference in sulfate and O_x dependence between 2015 and 2008 highlights the critical role of O_x in BSOA formation currently in the PRD.

In the revised manuscript, we add these discussion in line 324-332 “We further compared the results in 2015 with those during fall-winter season in 2008 at WQS (Ding et al., 2012). We found that all BSOA species positively correlated with sulfate but exhibited no O_x dependence (Table S7). Thus, in 2008 BSOA formation was largely influenced by sulfate, probably due to high sulfate levels then (as high as $46.8 \mu\text{g m}^{-3}$). Owing to strict control of SO_2 emissions (Wang et al., 2013), ambient SO_2 significantly shrank over the PRD (Figure 1b). Our long-term observation during fall-winter season at WQS also witnessed a decreasing trend of sulfate from 2007 to 2016 (Figure S10). However, O_x levels did not decrease during the past decade (Figure 1b) and O_x concentrations were much higher than sulfate in 2015 in the PRD ($96.1 \pm 14.9 \mu\text{g m}^{-3}$ vs. $8.44 \pm 1.09 \mu\text{g m}^{-3}$ on average). All these underline the importance of O_x in BSOA formation currently in the PRD.”

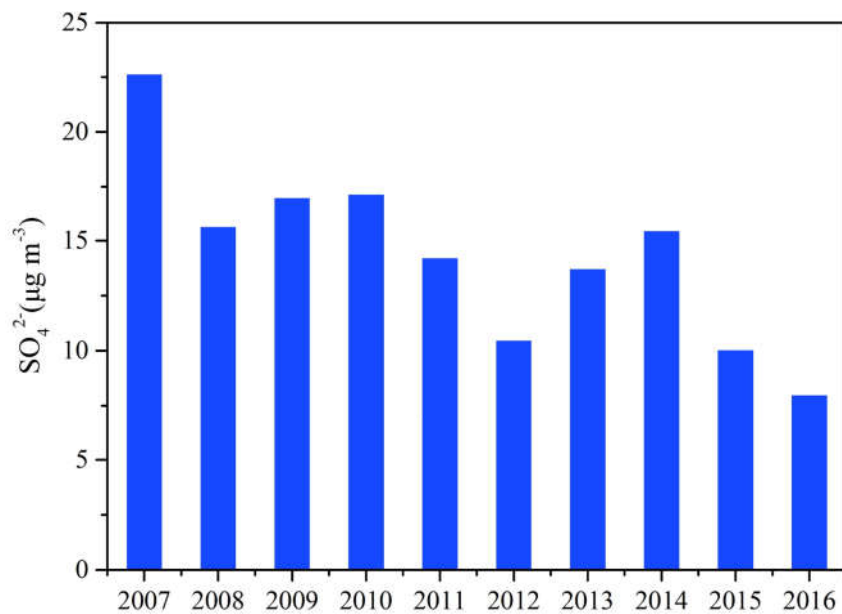


Figure R1-1 Long-term variation of sulfate in fall at WQS from 2007-2016.

Table R1-2 Correlations of BSOA with sulfate and O_x during fall-winter in 2008 at WQS

	Sulfate (2008-PRD)			O _x (2008-PRD)	
	Slope	<i>p</i> -value	% ^a	Slope	<i>p</i> -value
SOA _M	0.023	0.005	50	-	0.551
SOA _I	0.032	<0.001	76	-	0.509
SOA _C	0.032	<0.001	87	-	0.139
BSOA	0.087	<0.001	69	-	0.563

^a Percentages of SOA reduction at 50% decline of sulfate or O_x

Reference

Ding, X., Wang, X., Gao, B., Fu, X., He, Q., Zhao, X., Yu, J., and Zheng, M.: Tracer based estimation of secondary organic carbon in the Pearl River Delta, South China, *J. Geophys. Res-Atmos.*, 117, D05313, 10.1029/2011JD016596, 2012.

Minor Comments

1. Line 34. Replace “high-generation” with “later-generation” throughout the manuscript including acronyms.

Reply: We have replaced it as suggested. We also replace “SOA_{M,H}” with “SOA_{M,L}” throughout the

manuscript.

2. Line 231-232. The correlation between $\text{SOA}_{\text{M}_\text{H}}$ and sulfate is intriguing. The formation of $\text{SOA}_{\text{M}_\text{H}}$ tracers, like MBTCA, does not involve sulfate. Thus, how to explain the correlation?

Reply: Müller et al. (2012) reported that MBTCA could be formed through the gas-phase OH oxidation of pinonic acid. The triacid nature of MBTCA makes it highly water-soluble and able to partition into cloud water and aerosol liquid water (Aljawhary et al 2016). Besides the gas-phase OH oxidation, the heterogeneous OH oxidation of pinonic acid could also produce MBTCA (Lai et al. 2015). Aljawhary et al. (2016) reported the kinetics and mechanism of pinonic acid oxidation in acidic solutions and found that the molar yields of MBTCA through the aqueous-phase reactions were similar to those in the gas-phase oxidation. Sulfate is a key species in particles that determines aerosol liquid water amount, aerosol acidity, and particle surface area (Xu et al., 2015, 2016). Thus, the increase of sulfate could promote aqueous and heterogeneous reactions and produce substantial MBTCA in particles.

In the revised manuscript, we add these discussion in line 187-197 “On the other hand, sulfate is a key species in particles that determines aerosol liquid water amount, aerosol acidity, and particle surface area (Xu et al., 2015, 2016). Thus, the increase of sulfate could promote aqueous and heterogeneous reactions. In this study, the $\text{SOA}_{\text{M}_\text{F}}$ tracers poorly correlated with sulfate (Figure 5c), while the $\text{SOA}_{\text{M}_\text{L}}$ tracers positively correlated with sulfate at all the 9 sites (Figure 5d). At each site the $\text{SOA}_{\text{M}_\text{L}}$ tracers exhibited more sulfate dependence than $\text{SOA}_{\text{M}_\text{F}}$ tracers (Figure S5). This suggested that sulfate also played a critical role in forming $\text{SOA}_{\text{M}_\text{L}}$ tracers through the particle-phase reactions. Besides the gas-phase OH oxidation (Müller et al., 2012), the heterogeneous OH oxidation of pinonic acid could also produce $\text{SOA}_{\text{M}_\text{L}}$ tracers (Lai et al. 2015). Aljawhary et al., (2016) reported the kinetics and mechanism of pinonic acid oxidation in acidic solutions and found that the molar yields of MBTCA through the aqueous-phase reactions were similar to those in the gas-phase oxidation.”

Reference

1. Aljawhary, D., Zhao, R., Lee, A. K. Y., Wang, C., and Abbatt, J. P. D.: Kinetics, mechanism, and secondary organic aerosol yield of aqueous phase photo-oxidation of α -pinene oxidation products, J. Phys. Chem. A., 120, 1395-1407, 10.1021/acs.jpca.5b06237, 2016.
2. Lai, C., Liu, Y., Ma, J., Ma, Q., Chu, B., and He, H.: Heterogeneous kinetics of cis-pinonic acid with hydroxyl radical under different environmental conditions, J. Phys. Chem. A., 119, 6583-6593, 10.1021/acs.jpca.5b01321, 2015.
3. Müller, L., Reinnig, M. C., Naumann, K. H., Saathoff, H., Mentel, T. F., Donahue, N. M., and

Hoffmann, T.: Formation of 3-methyl-1,2,3-butanetricarboxylic acid via gas phase oxidation of pinonic acid – a mass spectrometric study of SOA aging, *Atmos. Chem. Phys.*, 12, 1483-1496, 10.5194/acp-12-1483-2012, 2012.

4. Xu, L., Guo, H., Boyd, C. M., Klein, M., Bougiatioti, A., Cerully, K. M., Hite, J. R., Isaacman-VanWertz, G., Kreisberg, N. M., Knote, C., Olson, K., Koss, A., Goldstein, A. H., Hering, S. V., de Gouw, J., Baumann, K., Lee, S.-H., Nenes, A., Weber, R. J., and Ng, N. L.: Effects of anthropogenic emissions on aerosol formation from isoprene and monoterpenes in the southeastern United States, *P. Natl. Acad. Sci. USA.*, 112, 37-42, 10.1073/P.Natl.Acad.Sci.USA.1417609112, 2015.

5. Xu, L., Middlebrook, A. M., Liao, J., de Gouw, J. A., Guo, H., Weber, R. J., Nenes, A., Lopez-Hilfiker, F. D., Lee, B. H., Thornton, J. A., Brock, C. A., Neuman, J. A., Nowak, J. B., Pollack, I. B., Welti, A., Graus, M., Warneke, C., and Ng, N. L.: Enhanced formation of isoprene-derived organic aerosol in sulfur-rich power plant plumes during Southeast Nexus, *J. Geophys. Res-Atmos.*, 121, 11137-11153, 10.1002/2016JD025156, 2016.

3. Please show the correlation of isoprene SOA tracers with sulfate and O_x , like figure 5.

Reply: As suggested, we checked the correlations of isoprene SOA tracers with sulfate and O_x (see below Figure R1-2) and added the figure into the Supporting Information as Figure S6. The NO/NO_2 -channel product exhibited more O_x and sulfate dependence than HO_2 -channel products. In the revised manuscript, we add these discussion in line 234-236 “We also checked the correlations of SOA_1 tracers with O_x and sulfate (Figure S6). The NO/NO_2 -channel product exhibited more O_x and sulfate dependence than HO_2 -channel products.”

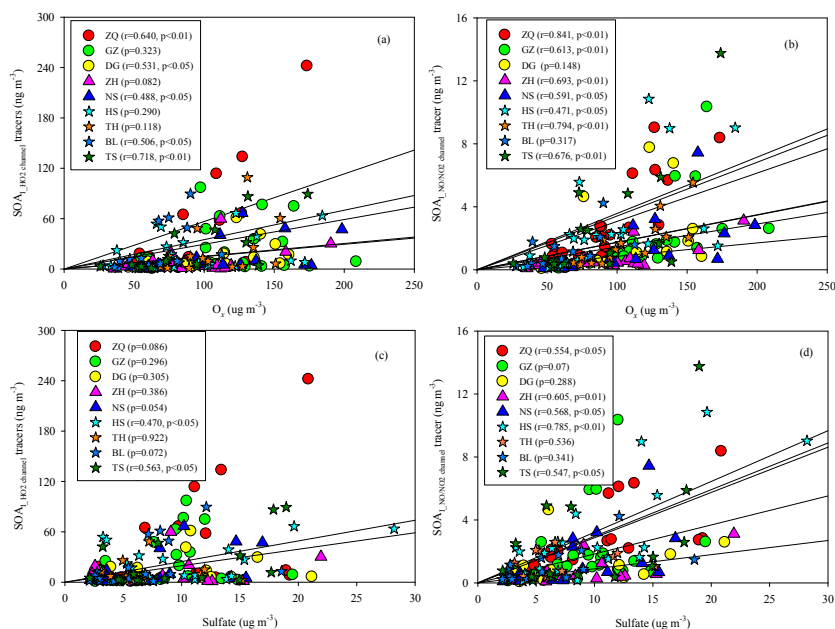
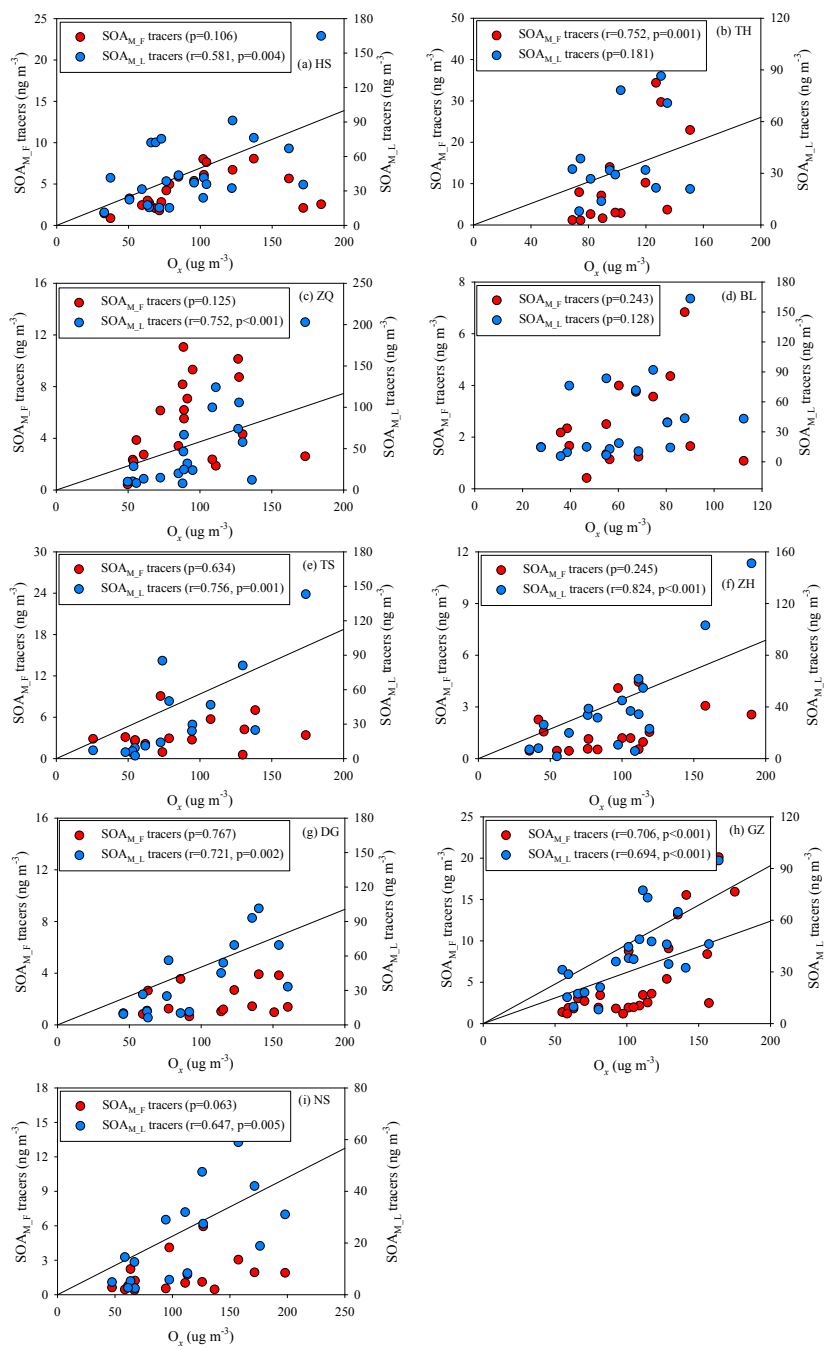


Figure R1-2 Correlations of $SOA_{HO2-channel}$ tracers and $SOA_{NO2-channel}$ tracers with O_3 (a, b) and sulfate (c, d)

4. Figure 5. With so many data on the plots, it is difficult to examine the correlation at each site. I suggest to make a scatter plot for each site and then synthesize a figure like figure 4.

Reply: As suggested, we add the scatter plots of SOA_{M-F} tracers and SOA_{M-L} tracers with O_3 and sulfate at each site in Supporting Information of the revised manuscript (Figure S4 and S5, see the Figure R1-3, R1-4 below).



176

177 Figure R1-3 Correlations of $\text{SOA}_{M,F}$ tracers and $\text{SOA}_{M,L}$ tracers with O_x

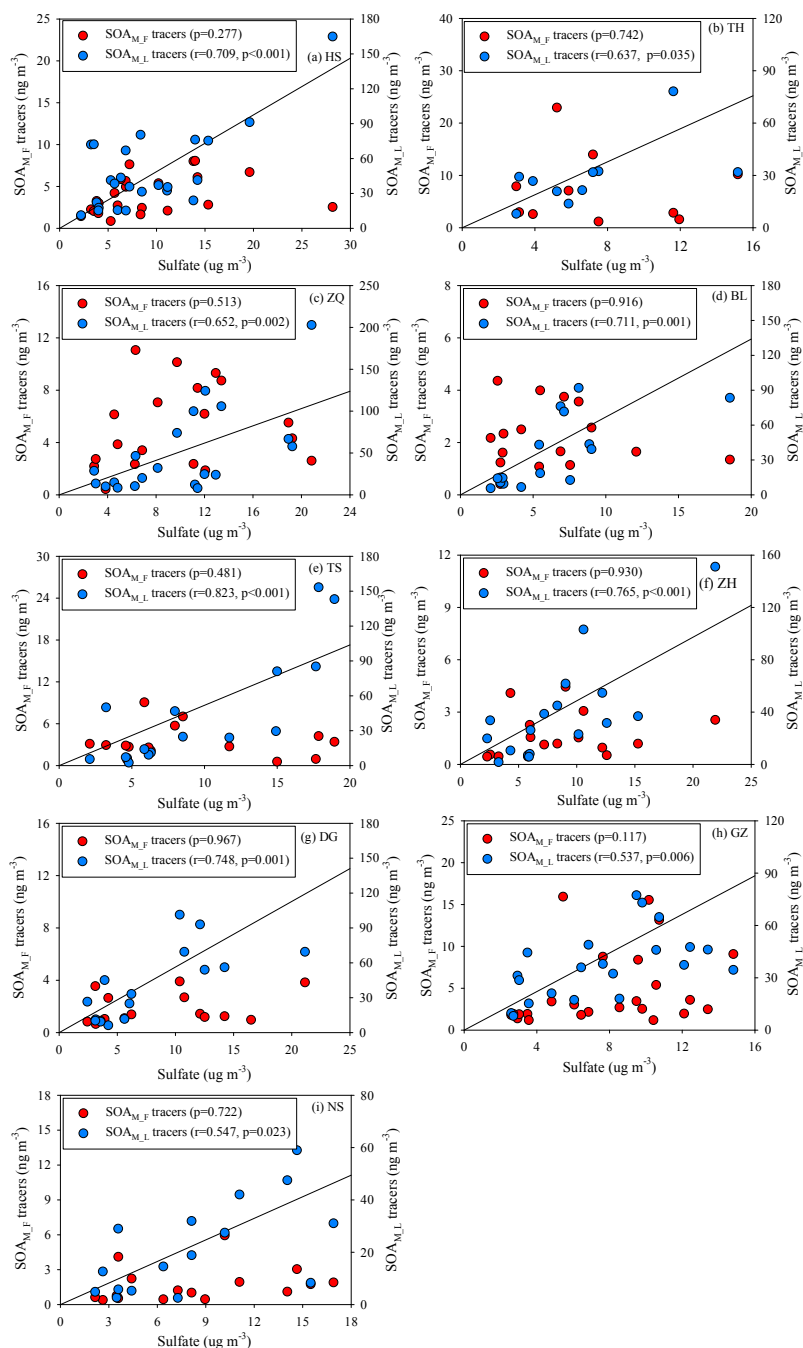


Figure R1-4 Correlations of $\text{SOA}_{M,F}$ tracers and $\text{SOA}_{M,L}$ tracers with sulfate

5. The correlation between β -caryophyllenic acid (CA) and levoglucosan is interesting. Does biomass burning emit CA?

Reply: To the best of our knowledge, biomass burning does not emit CA but its precursor. Sesquiterpenes, including β -caryophyllene are synthesized and stored in plant tissues partly to protect plants from insects and pathogens (Keeling and Bohlmann, 2006). When biomass burning events happen, high temperature could release substantial sesquiterpenes into the air (Ciccioli et al. 2014). On the other hand, the oxidation of β -caryophyllene by the OH radical and O_3 is very rapid. Under typical oxidation conditions in the air of PRD, the lifetimes of β -caryophyllene are only several minutes. This means that once emitted from biomass burning, β -caryophyllene could react rapidly and form CA immediately. Thus, it is expected to see a positive correlation between CA and levoglucosan.

In the revised manuscript, we add this discussion in Line 285-288 “The oxidation of β -caryophyllene by the OH radical and O_3 is very rapid. Under typical oxidation conditions in the air of PRD, the lifetimes of β -caryophyllene are only several minutes (Table S5). Once emitted from vegetation or biomass burning, β -caryophyllene will react rapidly and form CA immediately. This partly explains the positive correlations between CA and levoglucosan in the PRD.”

Reference

1. Keeling, C. I., and Bohlmann, J.: Genes, enzymes and chemicals of terpenoid diversity in the constitutive and induced defence of conifers against insects and pathogens, *New Phytol.*, 170, 657-675, 10.1111/j.1469-8137.2006.01716.x, 2006.
2. Ciccioli, P., Centritto, M., and Loreto, F.: Biogenic volatile organic compound emissions from vegetation fires, *Plant Cell Environ.*, 37, 1810-1825, 10.1111/pce.12336, 2014.

6. Line 331. The authors need to be careful about the salting-in effect, because it is highly compound-specific. Xu et al. 2015 proposed that sulfate introduces salting-in effect on IEPOX, but this is just a hypothesis. It would be overreaching to argue that sulfate has salting-in effect on β -caryophyllene SOA.

Reply: We agree. In the revised manuscript, we change the statement as “In addition, the increase of sulfate could raise aerosol acidity and thereby promote aqueous and heterogeneous reactions to form SOA_C.” in line 290-291.

Reviewer #2

This manuscript by Zhang et al. represent a detailed analysis on tracer organic compounds quantified in PM_{2.5} samples collected at 23 sites in the Pearl River Delta (PRD) region. Based on the tracer concentrations, the authors performed correlation analyses and source apportionment to understand the source of secondary organic aerosol (SOA), as well as the impact of anthropogenic emissions to biogenic SOA (BSOA). The topic of the study is timely and is within the scope of ACP. Especially, the interaction of anthropogenic and biogenic emissions in relatively polluted regions, such as the PRD, is not well understood, and the results from this study is highly valuable. The manuscript is of high quality in terms of chemical analysis, discussion, implication, and literary presentation. I recommend publication of this work in ACP and I have a number of minor and technical suggestions.

We thank the referee for the positive evaluation of our manuscript and the useful comments and suggestions. A point-by-point response is included below and we have revised the manuscript according to the comments.

1. - Section 2.2: The authors quantified quite a number of organic tracers. The authors should justify how representative are these tracers for SOA_I, SOA_M, and SOA_C. In particular, I am not familiar with HDMGA and HGA as tracers for monoterpenes. Citation is needed to justify the specificity and selectivity of these tracers.

Reply: For SOA_I tracers, Claeys et al (2004a) first identified 2-methyltetrols in Amazon aerosols and disclosed the importance of SOA_I. They further identified 2-methylglyceric acid (Claeys et al., 2004b) and C₅-alkene triols (Wang et al., 2005) as specific markers for acid-catalyzed ring opening of the isoprene-derived epoxides (e.g. MAE/HMML and IEPOXs). Lin et al., (2012) identified 3-MeTHF-3,4-diols as the products of acid-catalyzed intermolecular rearrangement of IEPOX on acidic particles.

For SOA_M tracers, pinic acid and pinonic acid were firstly identified in the chamber-generated SOA from the ozonolysis and OH oxidation of pinenes (Christoffersen et al 1998). Further oxidation of pinic acid and pinonic acid can form highly oxidized products, e.g. MBTCA whose chemical structure was finally identified by Szmigielski et al. (2007). 3-Hydroxyglutaric acid (HGA) and 3-hydroxy-4,4-dimethylglutaric acid (HDMGA) were first reported as SOA_M tracers (U1 and U2 compounds in the

Figure R2-1 below) by Claeys et al (2007). As a tracer for SOAc, β -Caryophyllenic acid was first identified by Jaoui et al. (2007).

In the revised manuscript, we add all these references to justify the specificity and selectivity of these tracers in Line 107-116.

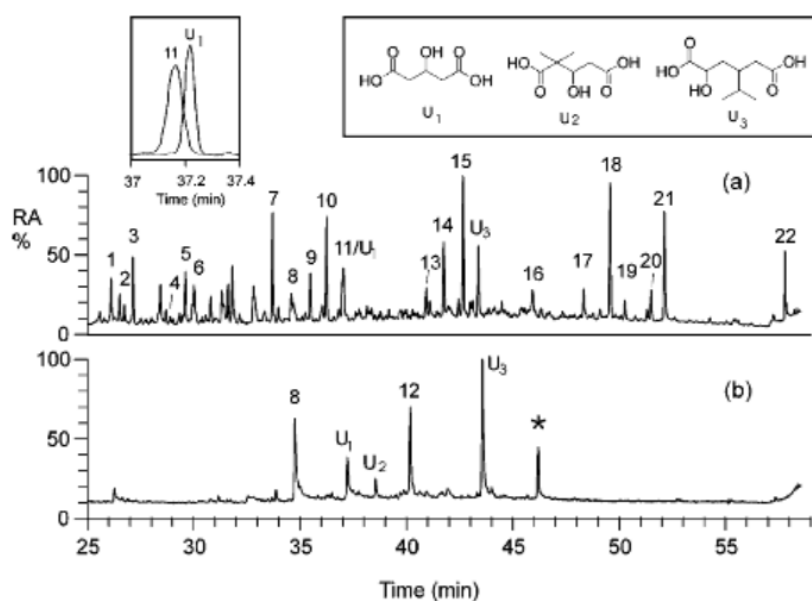


Figure R2-1 GC/MS TICs obtained for the trimethylsilylated extract of PM_{2.5} aerosols and the chemical structures of HGA (U1) and HDMGA (U2) from Claeys et al (2007).

Reference

1. Christoffersen, T. S., Hjorth, J., Horie, O., Jensen, N. R., Kotzias, D., Molander, L. L., Neeb, P., Ruppert, L., Winterhalter, R., Virkkula, A., Wirtz, K., and Larsen, B. R.: Cis-pinic acid, a possible precursor for organic aerosol formation from ozonolysis of α -pinene, *Atmos. Environ.*, 32, 1657-1661, [https://doi.org/10.1016/S1352-2310\(97\)00448-2](https://doi.org/10.1016/S1352-2310(97)00448-2), 1998.
2. Claeys, M., Graham, B., Vas, G., Wang, W., Vermeylen, R., Pashynska, V., Cafmeyer, J., Guyon, P., Andreae, M. O., Artaxo, P., and Maenhaut, W.: Formation of secondary organic aerosols through photooxidation of isoprene, *Science*, 303, 1173-1176, [10.1126/science.1092805](https://doi.org/10.1126/science.1092805), 2004a.
3. Claeys, M., Wang, W., Ion, A. C., Kourtchev, I., Gelencsér, A., and Maenhaut, W.: Formation of secondary organic aerosols from isoprene and its gas-phase oxidation products through reaction with hydrogen peroxide, *Atmos. Environ.*, 38, 4093-4098, <https://doi.org/10.1016/j.atmosenv.2004.06.001>, 2004b.
4. Claeys, M., Szmigielski, R., Kourtchev, I., Van der Veken, P., Vermeylen, R., Maenhaut, W., Jaoui, M., Kleindienst, T. E., Lewandowski, M., Offenberg, J. H., and Edney, E. O.: Hydroxydicarboxylic acids:

Markers for secondary organic aerosol from the photooxidation of α -pinene, *Environ. Sci. Technol.*, 41, 1628-1634, 10.1021/es0620181, 2007.

5. Jaoui, M., Lewandowski, M., Kleindienst, T. E., Offenberg, J. H., and Edney, E. O.: β -caryophyllinic acid: An atmospheric tracer for β -caryophyllene secondary organic aerosol, *Geophys. Res. Lett.*, 34, 10.1029/2006gl028827, 2007.

6. Lin, Y.-H., Zhang, Z., Docherty, K. S., Zhang, H., Budisulistiorini, S. H., Rubitschun, C. L., Shaw, S., Knipping, E., Edgerton, E. S., Kleindienst, T. E., Gold, A., and Surratt, J. D.: Isoprene epoxydiols as precursors to secondary organic aerosol formation: Acid-catalyzed reactive uptake studies with authentic standards, *Environ. Sci. Technol.*, 46, 189-195, 10.1021/es202554c, 2012.

7. Szmigielski, R., Surratt, J. D., Gómez-González, Y., Van der Veken, P., Kourtchev, I., Vermeylen, R., Blockhuys, F., Jaoui, M., Kleindienst, T. E., Lewandowski, M., Offenberg, J. H., Edney, E. O., Seinfeld, J. H., Maenhaut, W., and Claeys, M.: 3-methyl-1,2,3-butanetricarboxylic acid: An atmospheric tracer for terpene secondary organic aerosol, *Geophys. Res. Lett.*, 34, 10.1029/2007gl031338, 2007.

8. Wang, W., Kourtchev, I., Graham, B., Cafmeyer, J., Maenhaut, i., and Claeys, M.: Characterization of oxygenated derivatives of isoprene related to 2-methyltetrols in Amazonian aerosols using trimethylsilylation and gas chromatography/ion trap mass spectrometry, *Rapid Commun. Mass Spectrom.*, 19, 1343-1351, 10.1002/rcm.1940, 2005.

2. - Section 2.3: It seems that the recovery for erythritol is low. Why it is low and how is the result of the recovery test reflected in the quantification of related tracers?

Reply: In our study, apart from using internal standards, we also tested “absolute” recoveries for the standard compounds by analyzing spiked samples. The recovery results in QAQC showed the absolute recovery of each standard compound. Compared with PNA and octadecanoic acid, erythritol has the smallest carbon number and the lightest molecular weight. The loss of erythritol during chemical analysis should be highest among the three target compounds. Thus, the absolute recovery of erythritol is low.

For tracer quantification, we added internal standards to each sample before extraction and quantified SOA tracers using the internal standards approach. The internal calibration procedure uses the peak area ratio of target compound to internal standard to do the quantification. Since internal standards have similar chemical structure and/or retention time to the target compounds, their loss should be comparable to those of target compounds during sample analysis. The internal standard calibration based on peak area ratios is in fact already recovery corrected with the assumption that internal standards and target compounds have identical recoveries. Thus, the low absolute recovery of erythritol does not affect the quantification of related tracers.

3. - The authors use O_x as an indicator of the atmospheric oxidative capacity. However, caution is needed, as $O_x = (O_3 + NO_2)$ represents the total O_3 . While O_3 is certainly an important oxidant, the contribution

of OH radical (which is perhaps more important) is not considered in O_x . Is there any evidence showing that OH concentration is also high when the O_x concentration is high?

Reply: We admit that high O_x itself cannot indicate high oxidative capacity. In fact, Hofzumahaus et al., (2009) observed extremely high OH concentrations ($15 \times 10^6 \text{ cm}^{-3}$ around noon) in the PRD and proposed a recycling mechanism which increases the stability of OH in the air of polluted regions. Since O_3 , NO_x and OH are intimately linked in atmospheric chemistry, we think that the atmospheric oxidative capacity keeps high in the PRD. Because we did not have OH measurements in the current study, in the revised manuscript we remove the statement “ O_x as an indicator of the atmospheric oxidative capacity” and change the related discussion as:

“The SOA_C tracer elevated in winter at all sites and positively correlated with levoglucosan, O_x , and sulfate. Thus, the unexpected increase of SOA_C in wintertime might be highly associated with the enhancement of biomass burning, O_3 chemistry and sulfate component in the PRD.” (Line 31-34)

“However, O_3 and oxidant (O_x , $O_x = O_3 + NO_2$) are still in high levels and do not decrease apparently (Figure 1b). Hofzumahaus et al., (2009) observed extremely high OH concentrations in the PRD and proposed a recycling mechanism which increases the stability of OH in the air of polluted regions. All these indicate high atmospheric oxidative capacity in the PRD, since O_3 , NO_x and OH are intimately linked in atmospheric chemistry.” (Line 64-68)

“Due to the compromise of opposite seasonal trends of O_3 and NO_2 , O_x showed less seasonal variation (Figure 3f) compared with other gaseous pollutants. And annual-mean O_x reached $96.1 \pm 14.9 \mu\text{g m}^{-3}$. These indicated significant O_3 pollution all the year in the PRD.” (Line 147-150)

Reference

Hofzumahaus, A., Rohrer, F., Lu, K., Bohn, B., Brauers, T., Chang, C.-C., Fuchs, H., Holland, F., Kita, K., Kondo, Y., Li, X., Lou, S., Shao, M., Zeng, L., Wahner, A., and Zhang, Y.: Amplified trace gas removal in the troposphere, *Science*, 324, 1702-1704, 10.1126/science.1164566, 2009.

4. - Section 3.2.3: It is interesting that β -caryophyllenic acid (CA) was observed to be high in the winter and correlate with BB tracers. Can the authors comment on whether this observation place question on the selectivity and specificity of CA as a tracer for SOA_C ?

Reply: β -Caryophyllenic acid (CA) was identified in SOA produced through the ozonolysis and photooxidation of β -caryophyllene (Jaoui et al. 2007). Previous studies have demonstrate that biomass

burning does emit substantial sesquiterpenes (Ciccioli et al. 2014; Mentel et al., 2013) which are synthesized and stored in plant tissues to protect plants from insects and pathogens (Keeling and Bohlmann, 2006). On the other hand, the oxidation of β -caryophyllene in the air is very rapid. Under typical OH and O₃ levels in the air of PRD, the lifetimes of β -caryophyllene are only several minutes. Once emitted from biomass burning, β -caryophyllene could react rapidly and form CA immediately. Thus, it is expected to see a positive correlation between CA and levoglucosan. The unexpected high levels of CA in the winter indicated that biomass burning could be an important source of SOA_C in the PRD, especially in wintertime.

In the revised manuscript, we add this discussion in Line 285-290 “The oxidation of β -caryophyllene by the OH radical and O₃ is very rapid. Under typical oxidation conditions in the air of PRD, the lifetimes of β -caryophyllene are only several minutes (Table S5). Once emitted from vegetation or biomass burning, β -caryophyllene will react rapidly and form CA immediately. This partly explains the positive correlations between CA and levoglucosan in the PRD. The unexpected high levels of CA in the winter indicated that biomass burning could be an important source of SOA_C in the PRD, especially in wintertime.”

Reference

1. Ciccioli, P., Centritto, M., and Loreto, F.: Biogenic volatile organic compound emissions from vegetation fires, *Plant Cell Environ.*, 37, 1810-1825, 10.1111/pce.12336, 2014.
2. Jaoui, M., Lewandowski, M., Kleindienst, T. E., Offenberg, J. H., and Edney, E. O.: β -caryophyllinic acid: An atmospheric tracer for β -caryophyllene secondary organic aerosol, *Geophys. Res. Lett.*, 34, 10.1029/2006gl028827, 2007..
3. Keeling, C. I., and J. Bohlmann: Genes, enzymes and chemicals of terpenoid diversity in the constitutive and induced defence of conifers against insects and pathogens, *New Phytol.*, 170(4), 657–675, 2006.
4. Mentel, T. F., Kleist, E., Andres, S., Maso, M. D., Hohaus, T., Kiendler-Scharr, A., Rudich, Y., Springer, M., Tillmann, R., Uerlings, R., Wahner, A., and Wildt, J.: Secondary aerosol formation from stress-induced biogenic emissions and possible climate feedbacks, *Atmos. Chem. Phys.*, 13, 8755-8770, 10.5194/acp-13-8755-2013, 2013.
5. - Related to CA, I have come across compounds that have very similar names to β -caryophyllenic acid, namely, β -caryophyllinic acid and β -caryophyllonic acid. (Jaoui et al. (2007) *Geophys. Res. Lett.*; Bé et al. (2019) *ACS Earth Space Chem.*). Is β -caryophyllenic acid measured in this study a different compound or this is simply a typo?

Reply: β -Caryophyllenic acid, β -caryophyllinic acid and β -caryophyllonic acid in different studies are the same tracer of β -caryophyllene-derived SOA (see its chemical structure in the Figure R2-2 below). After derivatized with BSTFA, this compound has a molecular weight of 398 with fragment ions at m/z 383 and m/z 309 in the EI mass spectrum. Since there is a double-bond left, β -caryophyllenic acid is the accurate name.

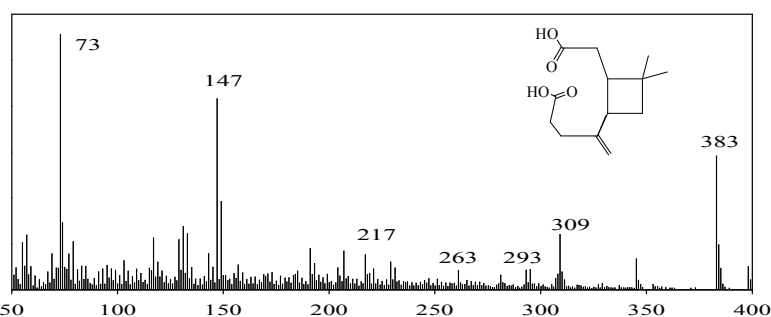


Figure R2-2 The GC/MS EICs obtained for the trimethylsilylated extract of PM_{2.5} aerosols and the chemical structure of β -caryophyllenic acid.

6. - Section 3.3: The impact of anthropogenic emissions to BSOA is perhaps one of the most important implications in this manuscript, but the current discussion appears weak. Based on the slopes obtained from the correlation studies, the authors implies that reducing SO₄ and O_x in the atmosphere will lead to reduction of BSOA. However, this type of correlation analysis exhibits only correlation but not causation. The authors should justify why reducing anthropogenic emissions can likely reduce BSOA. One way to do this, I think, is to add more discussion on the mechanisms behind the influence of anthropogenic emissions to BSOA.

Reply: Thanks for the suggestion. In the revised manuscript, we add more discussion on the mechanisms behind the influence of anthropogenic emissions to BSOA in Line 309-323 “It is interesting to note that SOA_M, SOA_I and SOA_C all positively correlated with sulfate and O_x in the PRD (Table 2). Since anthropogenic emissions can enhance BSOA formation (Hoyle et al., 2011), the reduction of anthropogenic emissions indeed lowers BSOA production (Carlton et al., 2018). As the oxidation product of SO₂, sulfate is a key species in particles that determines aerosol acidity and surface areas (Xu et al.,

2015, 2016) which could promotes BSOA formation through the acid-catalyzed heterogeneous reactions. Recent study found that SO₂ could directly reaction with organic peroxides of monoterpene ozonolysis and form substantial organosulfates (Ye et al., 2018). Thus, the decrease of SO₂ emission indeed reduces SO₂ and sulfate in the ambient air, which hereby leads to less acidic particles and reduces the BSOA production. For O_x, the increase of O₃ likely results in significant SOA formation through the BVOCs ozonolysis (Sipilä et al., 2014; Riva et al., 2017). Hence, the decrease of O_x resulting from the control of VOCs and NO_x emissions could reduce BSOA formation through O₃ chemistry. Based on the observed sulfate and O_x dependence of BSOA in this study, the reduction of 1 µg m⁻³ in sulfate and O_x in the air of PRD could lower BSOA levels by 0.17 and 0.02 µg m⁻³, respectively. If both concentrations decline by 50%, the reduction of O_x is more efficient than sulfate in reducing BSOA in the PRD (Table 2)."

Reference

1. Carlton, A. G., Pye, H. O. T., Baker, K. R., and Hennigan, C. J.: Additional benefits of federal air-quality rules: Model estimates of controllable biogenic secondary organic aerosol, *Environ. Sci. Technol.*, 52, 9254-9265, 10.1021/acs.est.8b01869, 2018.
2. Hoyle, C. R., Boy, M., Donahue, N. M., Fry, J. L., Glasius, M., Guenther, A., Hallar, A. G., Huff Hartz, K., Petters, M. D., Petäjä, T., Rosenoern, T., and Sullivan, A. P.: A review of the anthropogenic influence on biogenic secondary organic aerosol, *Atmos. Chem. Phys.*, 11, 321-343, 10.5194/acp-11-321-2011, 2011.
3. Riva, M., Budisulistiorini, S. H., Zhang, Z., Gold, A., Thornton, J. A., Turpin, B. J., and Surratt, J. D.: Multiphase reactivity of gaseous hydroperoxide oligomers produced from isoprene ozonolysis in the presence of acidified aerosols, *Atmos. Environ.*, 152, 314-322, 10.1016/j.atmosenv.2016.12.040, 2017.
4. Sipilä, M., Jokinen, T., Berndt, T., Richters, S., Makkonen, R., Donahue, N. M., Mauldin Iii, R. L., Kurtén, T., Paasonen, P., Sarnela, N., Ehn, M., Junninen, H., Rissanen, M. P., Thornton, J., Stratmann, F., Herrmann, H., Worsnop, D. R., Kulmala, M., Kerminen, V. M., and Petäjä, T.: Reactivity of stabilized Criegee intermediates (sCIs) from isoprene and monoterpene ozonolysis toward SO₂ and organic acids, *Atmos. Chem. Phys.*, 14, 12143-12153, 10.5194/acp-14-12143-2014, 2014.
5. Xu, L., Guo, H., Boyd, C. M., Klein, M., Bougiatioti, A., Cerully, K. M., Hite, J. R., Isaacman-VanWertz, G., Kreisberg, N. M., Knote, C., Olson, K., Koss, A., Goldstein, A. H., Hering, S. V., de Gouw, J., Baumann, K., Lee, S.-H., Nenes, A., Weber, R. J., and Ng, N. L.: Effects of anthropogenic emissions on aerosol formation from isoprene and monoterpenes in the southeastern United States, *P. Natl. Acad. Sci. USA.*, 112, 37-42, 10.1073/P.Natl.Acad.Sci.USA.1417609112, 2015.
6. Xu, L., Middlebrook, A. M., Liao, J., Gouw, J. A., Guo, H., Weber, R. J., Nenes, A., Lopez-Hilfiker, F. D., Lee, B. H., Thornton, J. A., Brock, C. A., Neuman, J. A., Nowak, J. B., Pollack, I. B., Welti, A., Graus, M., Warneke, C., and Ng, N. L.: Enhanced formation of isoprene-derived organic aerosol in sulfur-rich power plant plumes during Southeast Nexus, *J. Geophys. Res-Atmos.*, 121, 1137-1153, doi:10.1002/2016JD025156, 2016.
7. Ye, J., Abbatt, J. P. D., and Chan, A. W. H.: Novel pathway of SO₂ oxidation in the atmosphere: Reactions with monoterpene ozonolysis intermediates and secondary organic aerosol, *Atmos. Chem. Phys.*, 18, 5549-5565, 10.5194/acp-18-5549-2018, 2018.

Impact of anthropogenic emissions on biogenic secondary organic aerosol: Observation in the Pearl River Delta, South China

Yu-Qing Zhang^{1, *}, Duo-Hong Chen^{2, *}, Xiang Ding^{1, †}, Jun Li¹, Tao Zhang², Jun-Qi Wang¹, Qian Cheng¹, Hao Jiang¹, Wei Song¹, Yu-Bo Ou², Peng-Lin Ye³, Gan Zhang¹, Xin-Ming Wang^{1, 4}

¹ State Key Laboratory of Organic Geochemistry and Guangdong Provincial Key Laboratory of Environmental Protection and Resources Utilization, Guangzhou Institute of Geochemistry, Chinese Academy of Sciences, Guangzhou, 510640, China

² State Environmental Protection Key Laboratory of Regional Air Quality Monitoring, Environmental Monitoring Center of Guangdong Province, Guangzhou, 510308, China

³ Aerodyne Research Inc., Billerica, Massachusetts 01821, United States

⁴ Center for Excellence in Regional Atmospheric Environment, Institute of Urban Environment, Chinese Academy of Sciences, Xiamen, 361021, China

* These authors contributed equally to this work.

† Correspondence to: Xiang Ding (xiangd@gig.ac.cn)

429 **Abstract.** Secondary organic aerosol (SOA) formation from biogenic precursors is affected by
430 anthropogenic emissions, which is not well understood in polluted areas. In the study, we accomplished
431 a year-round campaign at nine sites in the polluted areas located in Pearl River Delta (PRD) region during
432 2015. We measured typical biogenic SOA (BSOA) tracers from isoprene, monoterpenes, and β -
433 caryophyllene as well as major gaseous and particulate pollutants and investigated the impact of
434 anthropogenic pollutants on BSOA formation. The concentrations of BSOA tracers were in the range of
435 45.4 to 109 ng m⁻³ with the majority composed of products from monoterpenes (SOA_M, 47.2 ± 9.29 ng
436 m⁻³), followed by isoprene (SOA_I, 23.1 ± 10.8 ng m⁻³), and β -caryophyllene (SOA_C, 3.85 ± 1.75 ng m⁻³).
437 We found that atmospheric oxidants, O_x (O₃ plus NO₂), and sulfate correlated well with later-generation
438 SOA_M tracers, but not so for first-generation SOA_M products. This suggested that high O_x and sulfate
439 could promote the formation of later-generation SOA_M products, which probably led to relatively aged
440 SOA_M we observed in the PRD. For the SOA_I tracers, not only 2-methylglyceric acid (NO/NO₂-channel
441 product), but also the ratio of 2-methylglyceric acid to 2-methyltetrols (HO₂-channel products) exhibit
442 NO_x dependence, indicating the significant impact of NO_x on SOA_I formation pathways. The SOA_C tracer
443 elevated in winter at all sites and positively correlated with levoglucosan, O_x, and sulfate. Thus, the
444 unexpected increase of SOA_C in wintertime might be highly associated with the enhancement of biomass
445 burning, O₃ chemistry and sulfate components in the PRD. The BSOAs that were estimated by the SOA
446 tracer approach showed the highest concentration in fall and the lowest concentration in spring with an
447 annual average concentration of 1.68 ± 0.40 μg m⁻³. SOA_M dominated the BSOA mass all year round.
448 We also found that BSOA correlated well with sulfate and O_x. This implicated the significant effects of
449 anthropogenic pollutants on BSOA formation and highlighted that we could reduce the BSOA through
450 controlling on the anthropogenic emissions of sulfate and O_x precursors in polluted regions.

删除的内容: high

删除的内容: high

删除的内容: atmospheric oxidation capacity

带格式的: 下标

451 1 Introduction

452 Secondary organic aerosols (SOA) that are produced through homogenous and heterogeneous processes
453 of volatile organic compounds (VOCs) have significant effects on global climate change and regional air
454 quality (von Schneidemesser et al., 2015). Globally, the emissions of biogenic VOCs (BVOCs) are
455 dominant over anthropogenic VOCs. Thus, biogenic SOA (BSOA) is predominant over anthropogenic
456 SOA. In the past decade, laboratorial, field, and modeling studies have demonstrated that BSOA

formation is highly affected by anthropogenic emissions (Zhang et al., 2015; Hoyle et al., 2011; Carlton et al., 2010). Increasing NO_x shifts isoprene oxidation from the low-NO_x conditions to the high-NO_x conditions (Surratt et al., 2010) and enhances nighttime SOA formation via nitrate radical oxidation of monoterpenes (Xu et al., 2015). High SO₂ emission leads to abundant sulfate and acidic particles, which accelerates the BSOA production by the salting-in effect and acid-catalyzed reactions (Offenberg et al., 2009; Xu et al., 2016). In polluted regions, the increase of O₃ levels due to high emissions of NO_x and VOCs, likely results in significant SOA formation through the ozonolysis of BVOCs (Sipilä et al., 2014; Riva et al., 2017). In addition, large emission and formation of anthropogenic organic matter (OM) in urban areas enhance the incorporation of BVOCs' oxidation products into the condensed phase (Donahue et al., 2006). Recently, Carlton et al. (2018) found that the removal of anthropogenic emissions of NO_x, SO₂, and primary OA in the CMAQ simulations could reduce BSOA by 23, 14, and 8% in summertime, respectively.

The Pearl River Delta region (PRD) (Figure 1a) is the most developed region in China. Rapid economic growth during the past three decades has resulted in large amounts of anthropogenic emissions in the PRD (Lu et al., 2013). Our observation during fall-winter season in 2008 at a regional site of the PRD showed that daily PM_{2.5} was as high as 150 µg m⁻³ (Ding et al., 2012). Fortunately, due to more and more strict and effective pollution controls in the PRD, PM_{2.5} concentrations have significantly shrunk during the last decade and met the national ambient air quality standard (NAAQS) for annual-mean PM_{2.5} (35 µg m⁻³) since the year of 2015 (Figure 1b). However, O₃ and oxidant (O_x, O_x = O₃ + NO₂) are still in high levels and do not decrease apparently (Figure 1b). ~~Hofzumahaus et al., (2009) observed extremely high OH concentrations in the PRD and proposed a recycling mechanism which increases the stability of OH in the air of polluted regions. All these indicate high atmospheric oxidative capacity in the PRD, since O₃, NO₂ and OH are intimately linked in atmospheric chemistry.~~ On the other hand, BVOCs emissions in the PRD are expected to be high all the year in such a subtropical area (Zheng et al., 2010). In the process of such a dramatic change in air pollution characteristics (e.g. PM_{2.5} and O₃), BSOA origins and formation mechanisms in the PRD should be profoundly affected in the last decade. In this study, year-round PM_{2.5} samples were collected at nine sites in the PRD during 2015. We investigated SOA tracers from typical BVOCs (isoprene, monoterpenes, and β-caryophyllene) across the PRD for the first time. We checked seasonal variations in concentrations and compositions of these BSOA tracers and evaluated the impact of anthropogenic pollutants on BSOAs formation in the PRD. We also accessed the

删除的内容: ,

删除的内容: indicating that atmospheric oxidative capacity in the PRD is still high (Hofzumahaus et al., 2009).

SOA origins and discussed the implication in further reducing BSOA through controlling on the anthropogenic emissions.

2 Experimental Section

2.1 Field Sampling

Concurrent sampling was performed at 9 out of 23 sites in the Guangdong-Hong Kong-Macao regional air quality monitoring network (<http://www.gdep.gov.cn/hjjce/>, Figure 1a), including three urban sites in Zhaoqing (ZQ), Guangzhou (GZ) and Dongguan (DG), two suburban sites in Nansha (NS) and Zhuhai (ZH), and four rural sites in Tianhu (TH), Boluo (BL), Heshan (HS) and Taishan (TS).

At each site, 24-hr sampling was conducted every six days from January to December in 2015 using a PM_{2.5} sampler equipped with quartz filters (8 × 10 inches) at a flow rate of 1.1 m³ min⁻¹. Additionally, field blanks were collected monthly at all sites. Blank filters were covered with aluminum foil and baked at 500 °C for 12 hrs and stored in a container with silica gel. After sampling, the filter samples were stored at -20 °C.

In this study, the filters collected in January, April, July and October 2015 were selected to represent winter, spring, summer, and fall samples, respectively. A total of 170 field samples (4-5 samples for each season at each site) were analyzed in the current study.

2.2 Chemical Analysis

For each filter, organic carbon (OC) and elemental carbon (EC) were measured by an OC-EC aerosol analyzer (Sunset Laboratory Inc.). Water-soluble ions were analyzed by ion chromatography (Metrohm). All these species are major components in PM_{2.5} (see Figure 2). Meteorological parameters (temperature and relative humidity) and gaseous pollutants (SO₂, CO, NO₂, NO, and O₃) at each site were recorded hourly. We further calculated the daily averages to probe the potential influence of air pollutants on BSOA formation.

For BSOA tracer analysis, detailed information of the processes is described in the previous literatures (Shen et al., 2015; Ding et al., 2012). Isotope-labeled standard mixtures, including dodecanoic acid-d₂₃, hexadecanoic acid-d₃₁, docosanoic acid-d₄₃ and levoglucosan-¹³C₆ were added into each sample as internal standards. Then, samples were extracted by sonication with the mixed solvents of dichloride methane (DCM)/hexane (1:1, v/v) and DCM/methanol (1:1, v/v), sequentially. The extraction solutions

of each sample were combined, filtered, and concentrated to ~2 mL. Each concentrated sample was split into two parts for silylation and methylation, respectively.

We analyzed fourteen BSOA tracers in the derivatized samples using GC/MSD (Agilent 7890/5975C). The isoprene-derived SOA (SOA_I) tracers were composed of 2-methyltetrols (2-MTLs, 2-methylthreitol and 2-methylerythritol) (Claeys et al., 2004a), 2-methylglyceric acid (2-MGA) (Claeys et al., 2004b), 3-MeTHF-3,4-diols (cis-3-methyltetrahydrofuran-3,4-diol and trans-3-methyltetrahydrofuran-3,4-diol) (Lin et al., 2012) and C₅-alkene triols (cis-2-methyl-1,3,4-trihydroxy-1-butene, trans-2-methyl-1,3,4-trihydroxy-1-butene and 3-methyl-2,3,4-trihydroxy-1-butene) (Wang et al., 2005). The monoterpenes-derived SOA (SOA_M) tracers included 3-hydroxy-4,4-dimethylglutaric acid (HDMGA), 3-hydroxyglutaric acid (HGA) (Claeys et al., 2007), pinic acid (PA), *cis*-pinonic acid (PNA) (Christoffersen et al., 1998), and 3-methyl-1,2,3-butanetricarboxylic acid (MBTCA) (Szmigielski et al., 2007). The β -caryophyllene-derived SOA (SOA_C) tracer was β -caryophyllenic acid (CA) (Jaoui et al., 2007). Due to the lack of authentic standards, surrogate standards were used to quantify BSOA tracers except PNA. Specifically, erythritol, PNA and octadecanoic acid were used for the quantification of SOA_I tracers (Ding et al., 2008), other SOA_M tracers (Ding et al., 2014) and CA (Ding et al., 2011), respectively. The method detection limits (MDLs) for erythritol, PNA and octadecanoic acid were 0.01, 0.02, and 0.02 ng m⁻³, respectively. Table S1 summarizes BSOA data at each site in the PRD.

2.3 Quality Assurance / Quality Control

These target BSOA tracers were not detected or lower than MDLs in the field blanks. The results of spiked samples (erythritol, PNA and octadecanoic acid spiked in pre-baked quartz filters) indicated that the recoveries were 65 \pm 14 % for erythritol, 101 \pm 3 % for PNA, and 83 \pm 7 % for octadecanoic acid. The results of paired duplicate samples indicated that all the relative differences for target BSOA tracers were lower than 15%.

It should be noted that the application of surrogate quantification introduces additional errors to the results. Based on the empirical approach to calculate uncertainties from surrogate quantification (Stone et al., 2012), we estimated the errors in analyte measurement which were propagated from the uncertainties in field blanks, spike recoveries, repeatability and surrogate quantification. As Table S2 showed, the estimated uncertainties in the tracers' measurement ranged from 15% (PNA) to 157% (CA).

删除的内容: 2-methyltetrols (2-MTLs, 2-methylthreitol and 2-methylerythritol),

3 Results and Discussion

3.1 PM_{2.5} and gaseous pollutants

Figure 2 presents spatial and seasonal variations of PM_{2.5} and its major components. Although annual-mean PM_{2.5} ($34.8 \pm 6.1 \mu\text{g m}^{-3}$) in the PRD met the NAAQS value of $35 \mu\text{g m}^{-3}$, PM_{2.5} at the urban sites (ZQ, GZ and DG) all exceeded the NAAQS value. The rural TH site in the northern part of PRD witnessed the lowest concentration of PM_{2.5} ($25.0 \mu\text{g m}^{-3}$) among the nine sites. PM_{2.5} levels were highest in winter (on average $60.1 \pm 21.6 \mu\text{g m}^{-3}$) and lowest in summer (on average $22.8 \pm 3.3 \mu\text{g m}^{-3}$). Carbonaceous aerosols and water-soluble ions together explained $98 \pm 11\%$ of PM_{2.5} masses. OM (OC \times 1.6) was the most abundant component in PM_{2.5}, followed by sulfate, ammonium, nitrate and EC. Similar to PM_{2.5}, the five major components all increased in winter and fall (Figure S1), suggesting severe PM_{2.5} pollution during fall-winter season in the PRD.

In the gas phase, SO₂, CO, NO₂ and NO_x presented similar seasonal trends as PM_{2.5}, i.e. higher levels occurred during fall and winter and lower concentrations during spring and summer (Figure 3 a-d). Annual-mean SO₂ and NO₂ in the PRD both met the NAAQS values of $60 \mu\text{g m}^{-3}$ and $40 \mu\text{g m}^{-3}$, respectively (Figure 3a and 3c). As a typical secondary pollutant, O₃ was highest in summer (Figure 3e), probably because of the strong photo-chemistry. Due to the compromise of opposite seasonal trends of O₃ and NO₂, O_x showed less seasonal variation (Figure 3f) compared with other gaseous pollutants. And annual-mean O_x reached $96.1 \pm 14.9 \mu\text{g m}^{-3}$. These indicated significant O₃ pollution all the year in the PRD.

删除的内容: These imply that atmospheric oxidative capacity is high all the year in the PRD.

3.2 Spatial distribution and seasonal variation of SOA tracers

The total concentrations of BSOA tracers ranged from 45.4 to 109 ng m⁻³ among the nine sites. SOA_M tracers ($47.2 \pm 9.29 \text{ ng m}^{-3}$) represented predominance, followed by SOA_I tracers ($23.1 \pm 10.8 \text{ ng m}^{-3}$), and SOA_C tracer ($3.85 \pm 1.75 \text{ ng m}^{-3}$).

3.2.1 Monoterpenes-derived SOA tracers

Annual averages of total SOA_M tracers at the nine sites were in the range of 26.5 to 57.4 ng m⁻³ (Table S1). Figure 4 and Figure S2a show the spatial distribution of SOA_M tracers and monoterpene emissions in the PRD (Zheng et al., 2010). The highest concentration of SOA_M tracers was observed at the rural TH site where monoterpene emissions were high. Figure 4 also presents seasonal variations of SOA_M

581 tracers. At most sites, high levels occurred in summer and fall. Monoterpene emission rates are
 582 influenced by temperature and solar radiation (Guenther et al., 2012). Thus, high temperature and
 583 intensive solar radiation during summer and fall in the PRD (Zheng et al., 2010) could stimulate
 584 monoterpene emissions and then the SOA_M formation.

585 Among the five SOA_M tracers, HGA ($20.1 \pm 4.28 \text{ ng m}^{-3}$) showed the highest concentration,
 586 followed by HDMGA ($14.7 \pm 2.93 \text{ ng m}^{-3}$), MBTCA ($7.63 \pm 1.49 \text{ ng m}^{-3}$), PNA ($3.75 \pm 2.72 \text{ ng m}^{-3}$) and
 587 PA ($1.01 \pm 0.48 \text{ ng m}^{-3}$). SOA_M formation undergoes multi-generation reactions. The first-generation
 588 SOA_M (SOA_{M_F}) products, PNA and PA, can be further oxidized and form the later-generation (SOA_{M_L})
 589 products, e.g. MBTCA (Müller et al., 2012). Thus, the (PNA+PA) / MBTCA ratio has been used to probe
 590 SOA_M aging (Haque et al., 2016; Ding et al., 2014). The (PNA+PA) / MBTCA ratios in chamber-
 591 generated α -pinene SOA samples were reported in the range of 1.51 to 5.91 depending on different
 592 oxidation conditions (Offenberg et al., 2007; Eddingsaas et al., 2012). In this study, the median values of
 593 (PNA+PA) / MBTCA varied from 0.27 at ZH to 1.67 at TH. The ratios observed in this study were
 594 consistent with our previous observations at the regional site, Wanqingsha (WQS) in the PRD (Ding et
 595 al., 2012), but lower than those in the fresh α -pinene SOA samples from chamber experiments (Figure
 596 S3), indicating relatively aged SOA_M in the air of PRD.

597 Moreover, the levels of SOA_{M_L} tracers (HGA + HDMGA + MBTCA) were much higher than those
 598 of SOA_{M_F} tracers (PNA + PA), with mean mass fractions of SOA_{M_L} tracers reaching 86% (Figure 4).
 599 Mass fractions of SOA_{M_F} tracers decreased in the summer samples (Figure 4), probably resulting from
 600 strong photo-chemistry and more intensive further oxidation during summer. High abundances of
 601 SOA_{M_L} tracers in the PRD were different from our year-round observations at 12 sites across China
 602 (Ding et al., 2016b). In that study, the (PNA+PA) / MBTCA ratio suggested generally fresh SOA_M (Figure
 603 S3) and SOA_{M_F} tracers were the majority. Thus, we see more aged SOA_M in the PRD.

604 As Figure 5 a-b and Figure S4,S5 showed, the SOA_{M_F} tracers did not show good correlations with
 605 O_x at most sites, while the SOA_{M_L} tracers exhibited significant O_x dependence. When O_x is high, strong
 606 photo-oxidation of PNA and PA could reduce their concentrations and promote the formation of SOA_{M_L}
 607 tracers (Müller et al., 2012). Thus, the levels of SOA_{M_L} tracers would increase with increasing O_x but
 608 not so for SOA_{M_F} tracers. On the other hand, sulfate is a key species in particles that determines aerosol
 609 liquid water amount, aerosol acidity and particle surface area (Xu et al., 2015, 2016). Thus, the increase
 610 of sulfate could promote aqueous and heterogeneous reactions. In this study, the SOA_{M_F} tracers poorly

删除的内容: high

删除的内容: H

删除的内容: g

删除的内容: H

删除的内容: H

删除的内容: H

删除的内容: H

删除的内容: atmospheric oxidation capacity

带格式的: 字体: 倾斜, 下标

删除的内容: H

删除的内容: H

删除的内容: and promotes SOA formation through the salting-in effect and heterogeneous reactions (Offenberg et al., 2009; Xu et al., 2016).

correlated with sulfate (Figure 5c), while the SOA_{M_L} tracers positively correlated with sulfate at all the 9 sites (Figure 5d). At each site the SOA_{M_L} tracers exhibited more sulfate dependence than the SOA_{M_F} tracers (Figure S5). This suggested that sulfate also played a critical role in forming SOA_{M_L} tracers through the particle-phase reactions. Besides the gas-phase OH oxidation (Müller et al., 2012), the heterogeneous OH oxidation of pinonic acid could also produce SOA_{M_L} tracers (Lai et al. 2015). Aljawhary et al., (2016) reported the kinetics and mechanism of pinonic acid oxidation in acidic solutions and found that the molar yields of MBTCA through the aqueous-phase reactions were similar to those in the gas-phase oxidation. Here, we conclude that high concentrations of O_x and sulfate could stimulate SOA_{M_L} tracers' production and thereby lead to aged SOA_M in the PRD.

3.2.2 Isoprene-derived SOA tracers

Annual averages of total SOA_I tracers at the nine sites were in the range of 10.8 to 49.3 ng m⁻³ (Table S1). Figure 6 and Figure S2b show the spatial distribution of SOA_I tracers and isoprene emissions in the PRD (Zheng et al., 2010), respectively. The highest concentration occurred at ZQ where the emissions were high. Figure 6 also presents seasonal variations of SOA_I tracers at the nine sites. High levels occurred in summer and fall. Similar to monoterpenes, the emission rate of isoprene is influenced by temperature and solar radiation (Guenther et al., 2012), which are expected to be higher in summer and fall in the PRD (Zheng et al., 2010). Among these SOA_I tracers, 2-MTLs (14.2 ± 5.61 ng m⁻³) were the most abundant products, followed by C₅-alkene triols (6.81 ± 5.05 ng m⁻³), 2-MGA (1.99 ± 0.72 ng m⁻³) and 3-MeTHF-3,4-diols (0.19 ± 0.08 ng m⁻³).

SOA_I formation is highly affected by NO_x (Surratt et al., 2010). Under the low-NO_x or NO_x free conditions, isoprene is oxidized by the OH and HO₂ radicals through the HO₂-channel which generates a hydroxy hydroperoxide (ISOPOOH) and then forms epoxydiols (IEPOX) (Paulot et al., 2009). Reactive uptake of IEPOX on acidic particles eventually produces 2-MTLs, C₅-alkene triols, 3-MeTHF-3,4-diols, 2-MTLs-organosulfates and oligomers (Lin et al., 2012). Under the high-NO_x conditions, isoprene undergoes oxidation by NO_x through the NO/NO₂-channel and generates methacrolein (MACR) and then forms peroxyethylacrylic nitric anhydride (MPAN). Further oxidation of MPAN by the OH radical produces hydroxymethyl-methyl-α-lactone (HMML) and/or methacrylic acid epoxide (MAE). HMML and MAE are the direct precursors to 2-MGA, 2-MGA-organosulfate and its corresponding oligomers (Nguyen et al., 2015). As Figure 6 showed, the concentrations of HO₂-channel tracers (2-MTLs + C₅-

删除的内容: The SOA_{M_F} tracers poorly correlated with sulfate (Figure 5c), while the SOA_{M_H} tracers presented significant sulfate dependence at all the 9 sites (Figure 5d). This suggested that sulfate also played a critical role in forming SOA_{M_H} tracers through particle phase reactions.

删除的内容: H

alkene triols + 3-MeTHF-3,4-diols) were much higher than those of the NO/NO₂-channel product (2-MGA) at all the nine sites. The dominance of HO₂-channel products was also observed at another regional site in the PRD (WQS) (He et al., 2018).

删除的内容: , largely due to strong heterogeneous reactions of IEPOXs on the acidic particles in the polluted air

Figure 6 also shows seasonal trends of the 2-MGA to 2-MTLs ratio (2-MGA/2-MTLs) which is often applied to probe the influence of NO_x on the formation of SOA_I (Ding et al., 2013; Ding et al., 2016a; Pye et al., 2013). The ratios were highest in wintertime and lowest in summertime, which were consistent with the seasonal trend of NO_x during our campaign (Figure 3d). As Table 1 showed, 2-MGA positively correlated with NO₂, probably due to the enhanced formation of MPAN from peroxyethacryloyl (PMA) radical reacted with NO₂ (Worton et al., 2013; Chan et al., 2010). Previous laboratory studies showed that increasing NO₂/NO ratio could promote the formation of 2-MGA and its corresponding oligoesters (Chan et al., 2010; Surratt et al., 2010). However, we did not see a significant correlation between 2-MGA and NO₂/NO ratio in the PRD. Instead, the 2-MGA/2-MTLs ratio correlated well with NO, NO₂ and NO₂/NO ratio (Table 1). Increasing NO limits the formation of ISOPOOH but prefers the production of MACR, and increasing NO₂ enhances MPAN formation. Thus, it is expected that the 2-MGA/2-MTLs ratio shows stronger NO_x dependence than 2-MGA. These findings demonstrate the significant impact of NO_x on SOA_I formation pathways in the atmosphere. We also checked the correlations of SOA_I tracers with O₃ and sulfate (Figure S6). The NO/NO₂-channel product exhibited more O₃ and sulfate dependence than HO₂-channel products.

带格式的: 字体颜色: 自动设置

Recent studies indicated that isoprene ozonolysis might play a role in SOA_I formation in the ambient air. Riva et al. (2016) found that isoprene ozonolysis with acidic particles could produce substantial 2-MTLs but not so for C₅-alkene triols and 3-MeTHF-3,4-diols. Li et al. (2018) observed a positive correlation between 2-MTLs and O₃ in the North China Plain. In the PRD, we also saw weak but significant correlations of 2-MTLs with O₃ (Table S3). However, 3-MeTHF-3,4-diols and C₅-alkene triols were detected in all samples and 2-MTLs, C₅-alkene triols and 3-MeTHF-3,4-diols correlated well with each other (Table S4), which was apparently different from those reported by Riva et al. (2016). Moreover, the ratios of 2-MTLs isomers in the PRD samples (2.00–2.85) were much lower than those (10–22, Figure S7) reported in the SOA from isoprene ozonolysis (Riva et al., 2016). Furthermore, isoprene oxidation by the OH radical is much faster than that by ozone under the polluted PRD conditions (Table S5). And IEPOX yields through the ISOPOOH oxidation by the OH radical are more than 75% in the atmosphere (St. Clair et al., 2016). Thus, isoprene ozonolysis might be not the major formation

删除的内容: 4

pathway of SOA₁, even though annual-mean O₃ level reaching 67.7 μg m⁻³ in the PRD (Table S1).

Previous studies found that thermal decomposition of low volatility organics in IEPOX-derived SOA could produce SOA₁ tracers, e.g. 2-MTLs, C₅-alkene triols and 3-MeTHF-3,4-diols (Lopez-Hilfiker et al., 2016, Watanabe et al., 2018). This means that these tracers detected by GC-MSD might be generated from thermal decomposition of IEPOX-derived SOA. As estimated by Cui et al (2018), 14.7-42.8% of C₅-alkene triols, 11.1% of 2-MTLs and approximately all 3-MeTHF-3,4-diols measured by GC/MSD could be attributed to the thermal degradation of 2-MTLs-derived organosulfates (MTL-OSs). We also measured MTL-OSs in two samples at HS and TS sites, respectively (Table S6) using the widely used LC-MS approach (He et al., 2014, 2018). Assuming that all MTL-OSs decomposed to these tracers, the thermal decomposition of MTL-OSs would account for 15.1-31.6% of C₅-alkene triols, 6.0-10.0% of 2-MTLs and all 3-MeTHF-3,4-diols measured by GC/MSD. Thus, C₅-alkene triols and 2-MTLs are major from isoprene oxidation rather than thermal decomposition of MTL-OSs, while 3-MeTHF-3,4-diols are only in trace amount in the air and might be produced largely from thermal degradation.

Moreover, we see significant variations in SOA₁ tracer compositions in the PRD. For instant, C₅-alkene triols have three isomers. If these tracers were mainly generated from a thermal process, their compositions should be similar in different samples. In fact, the relative abundances of three C₅-alkene triol isomers significantly changed from site to site (Figure 7) and season to season (Figure S8), and their compositions in the PRD were different from those measured in the chamber samples (Lin et al., 2012). In addition, the slopes of linear correlations among these IEPOX-derived SOA tracers also varied from site to site (Figure S9). Coupled with the seasonal trend of 2-MGA/2-MTLs ratios, the apparent variations in SOA₁ tracer compositions demonstrate that these SOA₁ tracers are mainly formed through different pathways in the ambient atmosphere, although part of them might arise from the thermal decomposition of different dimers/OSs and the parent dimers/OSs varies with sites and seasons.

3.2.3 Sesquiterpene-derived SOA tracer

Annual averages of CA at the nine sites ranged from 1.82 to 7.07 ng m⁻³. The levels of CA at the inland sites (e.g. GZ, ZQ, and TH) were higher than those at the coastal sites (ZH and NS, Figure 8). Since sesquiterpenes are typical BVOCs, it is unexpected that the concentrations of CA were highest during winter in the PRD (Figure 8). Interestingly, seasonal trend of CA was consistent with that of the biomass burning (BB) tracer, levoglucosan (Figure 8). And CA correlated well with levoglucosan at eight sites in

删除的内容: A previous study found that thermal decomposition of low volatility organics in IEPOX-derived SOA could produce SOA₁ tracers, e.g. 2-MTLs, C₅-alkene triols and 3-MeTHF-3,4-diols (Lopez-Hilfiker et al., 2016). This means that these tracers detected by GC-MSD might be generated from thermal decomposition of IEPOX-derived SOA. If these tracers were mainly generated from such a thermal process, their compositions would be similar in different samples. To verify this possibility, we presented chemical compositions of three C₅-alkene triol isomers at the nine sites in ternary plots. The relative abundances of three isomers significantly changed from site to site (Figure 7) and season to season (Figure S5), and were different from those measured in the chamber samples (Lin et al., 2012). Moreover, the slopes of linear correlations among these IEPOX-derived SOA tracers also varied from site to site (Figure S6). Coupled with the seasonal trend of 2-MGA/2-MTLs ratios, the observed variations in SOA₁ tracers compositions demonstrated that the SOA₁ tracers were mainly formed through different pathways in the real atmosphere rather than thermal decomposition. .

the PRD (Figure 9a). Sesquiterpenes are stored in plant tissues partly to protect the plants from insects and pathogens (Keeling and Bohlmann, 2006). BB can not only stimulate sesquiterpene emissions (Ciccioli et al., 2014) but also substantially alter the SOA formation and yields (Mentel et al., 2013). Emissions inventories in the PRD showed that the BB emissions were enhanced during winter (He et al., 2011). These suggested that the unexpected increase of SOA_C in wintertime could be highly associated with BB emissions in the PRD.

Besides the impact of BB, we also found positive correlations of CA with O_x (Figure 9b) and sulfate (Figure 9c). The oxidation of β-caryophyllene by the OH radical and O₃ is very rapid. Under typical oxidation conditions in the air of PRD, the lifetimes of β-caryophyllene are only several minutes (Table S5). Once emitted from vegetation or biomass burning, β-caryophyllene will reacted rapidly and form CA immediately. This partly explains the positive correlations between CA and levoglucosan in the PRD. The unexpected high levels of CA in the winter indicated that biomass burning could be an important source of SOA_C in the PRD, especially in wintertime. In addition, the increase of sulfate could raise aerosol acidity and thereby promote aqueous and heterogeneous reactions to form SOA_C. In the PRD, both O_x (Figure 3f) and sulfate (Figure S1) increased during winter, which could promote SOA_C formation. Here, we conclude that the enhancement of BB emissions as well as the increase of O_x and sulfate in wintertime together led to high SOA_C production during winter in the PRD.

3.3 Source apportionment and atmospheric implications

We further attributed BSOA by the SOA-tracer approach which was first developed by Kleindienst et al. (2007). This method has applied to SOA apportionment at multiple sites across the United States (Lewandowski et al., 2013) and China (Ding et al., 2016b), and over global oceans from Arctic to Antarctic (Hu et al., 2013). Details of the SOA-tracer method and its application in this study as well as the uncertainty of estimating procedure are described in Text S1. Table S1 lists the results of estimated SOA from different BVOCs.

Figure 10a exhibits the spatial distribution of BSOA (SOA_M + SOA_I + SOA_C). Annual average at the nine sites ranged from 0.97 μg m⁻³ (NS) to 2.19 μg m⁻³ (ZQ), accounting for 9-15% of OM. SOA_M was the largest BSOA contributor with an average contribution of 64 ± 7 %, followed by SOA_C (21 ± 6 %), and SOA_I (14 ± 4 %). Figure 10b presents seasonal variation of BSOA. The levels were highest in fall (2.35 ± 0.95 μg m⁻³) and lowest in spring (1.06 ± 0.42 μg m⁻³). SOA_M contributions ranged from 57%

删除的内容: The oxidation of β-caryophyllene by the OH radical and O₃ is very rapid with the lifetimes less than 10 min under typical conditions in the air of PRD (Table S5). The increase of sulfate could not only raise aerosol acidity but also enhance the salting-in effect (Xu et al., 2015). In the PRD, both O_x (Figure 3f) and sulfate (Figure S1) increased during winter, which could promote SOA_C formation.

in winter to 68% in spring. The shares of SOA_I were only 5% in winter and reached up to 22% in summer. The contributions of SOA_C increased to 40% in wintertime.

It is interesting to note that SOA_M, SOA_I and SOA_C all positively correlated with sulfate and O_x in the PRD (Table 2). Since anthropogenic emissions can enhance BSOA formation (Hoyle et al., 2011), the reduction of anthropogenic emissions indeed lowers BSOA production (Carlton et al., 2018). As the oxidation product of SO₂, sulfate is a key species in particles that determines aerosol acidity and surface areas (Xu et al., 2015, 2016) which could promotes BSOA formation through the acid-catalyzed heterogeneous reactions. Recent study found that SO₂ could directly reaction with organic peroxides of monoterpene ozonolysis and form substantial organosulfates (Ye et al., 2018). Thus, the decrease of SO₂ emission indeed reduces SO₂ and sulfate in the ambient air, which hereby leads to less acidic particles and reduces the BSOA production. For O_x, the increase of O₃ likely results in significant SOA formation through the BVOCs ozonolysis (Sipilä et al., 2014; Riva et al., 2017). Hence, the decrease of O_x resulting from the control of VOCs and NO_x emissions could reduce BSOA formation through O₃ chemistry. Based on the observed sulfate and O_x dependence of BSOA in this study, the reduction of 1 µg m⁻³ in sulfate and O_x in the air of PRD could lower BSOA levels by 0.17 and 0.02 µg m⁻³, respectively. If both concentrations decline by 50%, the reduction of O_x is more efficient than sulfate in reducing BSOA in the PRD (Table 2).

We further compared the results in 2015 with those during fall-winter season in 2008 at WQS (Ding et al., 2012). We found that all BSOA species positively correlated with sulfate but exhibited no O_x dependence (Table S7). Thus, in 2008 BSOA formation was largely influenced by sulfate, probably due to high sulfate levels then (as high as 46.8 µg m⁻³). Owing to strict control of SO₂ emissions (Wang et al., 2013), ambient SO₂ significantly shrank over the PRD (Figure 1b). Our long-term observation during fall-winter season at WQS also witnessed a decreasing trend of sulfate from 2007 to 2016 (Figure S10). However, O_x levels did not decrease during the past decade (Figure 1b) and O_x concentrations were much higher than sulfate in 2015 in the PRD (96.1 ± 14.9 µg m⁻³ vs. 8.44 ± 1.09 µg m⁻³ on average). All these underline the importance of O_x in BSOA formation currently in the PRD. At present, short-term despiking and long-term attainment of O₃ concentrations are challenges for air pollution control in the PRD (Ou et al., 2016). Thus, lowering O_x is critical to improve air quality in the PRD. Our results highlight the importance of future reduction in anthropogenic pollutant emissions (e.g. SO₂ and O_x precursors) for considerably reducing the BSOA burden in polluted regions.

删除的内容: Anthropogenic emissions significantly influence BSOA formation (Carlton et al., 2018). The observed sulfate and O_x dependence of BSOA in the air of PRD indicates that the reduction of 1 µg m⁻³ in sulfate and O_x could lower BSOA levels by 0.17 and 0.02 µg m⁻³, respectively. If both concentrations decline by 50%, the reduction of O_x is more efficient than sulfate in reducing BSOA in the PRD (Table 2). Due to strict control of SO₂ emissions (Wang et al., 2013), ambient SO₂ significantly shrank over the PRD (Figure 1b). However, O_x levels did not decrease during the past decade (Figure 1b) and O_x concentrations were much higher than sulfate in the PRD (96.1 ± 14.9 µg m⁻³ vs. 8.44 ± 1.09 µg m⁻³ on average).

Code/Data availability

The experimental data in this study are available upon request to the corresponding author by email.

Author Contribution

Xiang Ding, Duo-Hong Chen and Jun Li conceived the project and designed the study. Yu-Qing Zhang and Duo-Hong Chen performed the data analysis and wrote the manuscript. Duo-Hong Chen, Tao Zhang and Yu-Bo Ou arranged the sample collection and assisted with the data analysis. Jun-Qi Wang, Qian Cheng and Hao Jiang analyzed the samples. Xiang Ding, Peng-Lin Ye, Wei Song, Gan Zhang and Xin-Ming Wang performed data interpretation and edited the manuscript. All authors contributed to the final manuscript development.

Competing interests

The authors declare that they have no conflict of interest.

Acknowledgments

This study was supported by National Key Research and Development Program (2018YFC0213902), National Natural Science Foundation of China (41722305/41603070/41473099), and Local Innovative and Research Teams Project of Guangdong Pearl River Talents Program (NO. 2017BT01Z134). [We would like to thank Prof. Sasho Gligorovski for his helpful suggestion on the discussion of atmospheric oxidation process.](#) The data of gaseous pollutants, major components in PM_{2.5} and BSOA tracers can be found in supporting information.

References

- [Aljawhary, D., Zhao, R., Lee, A. K. Y., Wang, C., and Abbatt, J. P. D.: Kinetics, mechanism, and secondary organic aerosol yield of aqueous phase photo-oxidation of \$\alpha\$ -pinene oxidation products, *J. Phys. Chem. A*, **120**, 1395-1407, 10.1021/acs.jpca.5b06237, 2016.](#)
- Carlton, A. G., Pinder, R. W., Bhavsar, P. V., and Pouliot, G. A.: To what extent can biogenic SOA be controlled?, *Environ. Sci. Technol.*, **44**, 3376-3380, 10.1021/es903506b, 2010.
- Carlton, A. G., Pye, H. O. T., Baker, K. R., and Hennigan, C. J.: Additional benefits of federal air-quality

846 rules: Model estimates of controllable biogenic secondary organic aerosol, *Environ. Sci. Technol.*, 52,
847 9254-9265, 10.1021/acs.est.8b01869, 2018.

848 Chan, A. W. H., Chan, M. N., Surratt, J. D., Chhabra, P. S., Loza, C. L., Crounse, J. D., Yee, L. D., Flagan,
849 R. C., Wennberg, P. O., and Seinfeld, J. H.: Role of aldehyde chemistry and NO_x concentrations in
850 secondary organic aerosol formation, *Atmos. Chem. Phys.*, 10, 7169-7188, 10.5194/acp-10-7169-
851 2010, 2010.

852 [Christoffersen, T. S., Hjorth, J., Horie, O., Jensen, N. R., Kotzias, D., Molander, L. L., Neeb, P., Ruppert,](#)
853 [L., Winterhalter, R., Virkkula, A., Wirtz, K., and Larsen, B. R.: Cis-pinic acid, a possible precursor for](#)
854 [organic aerosol formation from ozonolysis of \$\alpha\$ -pinene, *Atmos. Environ.*, 32, 1657-1661,](#)
855 [https://doi.org/10.1016/S1352-2310\(97\)00448-2](https://doi.org/10.1016/S1352-2310(97)00448-2), 1998.

856 Ciccioli, P., Centritto, M., and Loreto, F.: Biogenic volatile organic compound emissions from vegetation
857 fires, *Plant Cell Environ.*, 37, 1810-1825, 10.1111/pce.12336, 2014.

858 [Claeys, M., Graham, B., Vas, G., Wang, W., Vermeylen, R., Pashynska, V., Cafmeyer, J., Guyon, P.,](#)
859 [Andreae, M. O., Artaxo, P., and Maenhaut, W.: Formation of secondary organic aerosols through](#)
860 [photooxidation of isoprene, *Science*, 303, 1173-1176, 10.1126/science.1092805, 2004a.](#)

861 [Claeys, M., Wang, W., Ion, A. C., Kourchev, I., Gelencsér, A., and Maenhaut, W.: Formation of](#)
862 [secondary organic aerosols from isoprene and its gas-phase oxidation products through reaction with](#)
863 [hydrogen peroxide, *Atmos. Environ.*, 38, 4093-4098, https://doi.org/10.1016/j.atmosenv.2004.06.001,](#)
864 [2004b.](#)

865 [Claeys, M., Szmigielski, R., Kourchev, I., Van der Veken, P., Vermeylen, R., Maenhaut, W., Jaoui, M.,](#)
866 [Kleindienst, T. E., Lewandowski, M., Offenberg, J. H., and Edney, E. O.: Hydroxydicarboxylic acids:](#)
867 [Markers for secondary organic aerosol from the photooxidation of \$\alpha\$ -pinene, *Environ. Sci. Technol.*,](#)
868 [41, 1628-1634, 10.1021/es0620181, 2007.](#)

869 [Cui, T., Zeng, Z., dos Santos, E. O., Zhang, Z., Chen, Y., Zhang, Y., Rose, C. A., Budisulistiorini, S. H.,](#)
870 [Collins, L. B., Bodnar, W. M., de Souza, R. A. F., Martin, S. T., Machado, C. M. D., Turpin, B. J.,](#)
871 [Gold, A., Ault, A. P., and Surratt, J. D.: Development of a hydrophilic interaction liquid](#)
872 [chromatography \(HILIC\) method for the chemical characterization of water-soluble isoprene](#)
873 [epoxydiol \(IEPOX\)-derived secondary organic aerosol, *Environ. Sci.: Processes Impacts*, 20, 1524-](#)
874 [1536, 10.1039/C8EM00308D, 2018.](#)

875 Ding, X., Zheng, M., Yu, L., Zhang, X., Weber, R. J., Yan, B., Russell, A. G., Edgerton, E. S., and Wang,

删除的内容: .

删除的内容: .

878 X.: Spatial and seasonal trends in biogenic secondary organic aerosol tracers and water-soluble organic
879 carbon in the southeastern United States, *Environ. Sci. Technol.*, 42, 5171-5176, 10.1021/es7032636,
880 2008.

881 Ding, X., Wang, X., and Zheng, M.: The influence of temperature and aerosol acidity on biogenic
882 secondary organic aerosol tracers: Observations at a rural site in the central Pearl River Delta region,
883 South China, *Atmos. Environ.*, 45, 1303-1311, 10.1016/j.atmosenv.2010.11.057, 2011.

884 Ding, X., Wang, X., Gao, B., Fu, X., He, Q., Zhao, X., Yu, J., and Zheng, M.: Tracer based estimation of
885 secondary organic carbon in the Pearl River Delta, South China, *J. Geophys. Res-Atmos.*, 117, D05313,
886 10.1029/2011JD016596, 2012.

887 Ding, X., Wang, X., Xie, Z., Zhang, Z., and Sun, L.: Impacts of Siberian biomass burning on organic
888 aerosols over the North Pacific Ocean and the Arctic: Primary and secondary organic tracers, *Environ.*
889 *Sci. Technol.*, 47, 3149-3157, 10.1021/es3037093, 2013.

890 Ding, X., He, Q. F., Shen, R. Q., Yu, Q. Q., and Wang, X. M.: Spatial distributions of secondary organic
891 aerosols from isoprene, monoterpenes, β -caryophyllene, and aromatics over China during summer, *J.*
892 *Geophys. Res-Atmos.*, 119, 11877-11891, 10.1002/2014JD021748, 2014.

893 Ding, X., He, Q. F., Shen, R. Q., Yu, Q. Q., Zhang, Y. Q., Xin, J. Y., Wen, T. X., and Wang, X. M.: Spatial
894 and seasonal variations of isoprene secondary organic aerosol in China: Significant impact of biomass
895 burning during winter, *Sci. Rep.*, 6, 20411, 10.1038/srep20411, 2016a.

896 Ding, X., Zhang, Y. Q., He, Q. F., Yu, Q. Q., Shen, R. Q., Zhang, Y., Zhang, Z., Lyu, S. J., Hu, Q. H.,
897 Wang, Y. S., Li, L. F., Song, W., and Wang, X. M.: Spatial and seasonal variations of secondary organic
898 aerosol from terpenoids over China, *J. Geophys. Res-Atmos.*, 121, 14661-14678,
899 10.1002/2016JD025467, 2016b.

900 Donahue, N. M., Robinson, A. L., Stanier, C. O., and Pandis, S. N.: Coupled partitioning, dilution, and
901 chemical aging of semivolatile organics, *Environ. Sci. Technol.*, 40, 2635-2643, 10.1021/es052297c,
902 2006.

903 Eddingsaas, N. C., Loza, C. L., Yee, L. D., Chan, M., Schilling, K. A., Chhabra, P. S., Seinfeld, J. H., and
904 Wennberg, P. O.: α -pinene photooxidation under controlled chemical conditions – Part 2: SOA yield
905 and composition in low- and high-NO_x environments, *Atmos. Chem. Phys.*, 12, 7413-7427,
906 10.5194/acp-12-7413-2012, 2012.

907 Guenther, A. B., Jiang, X., Heald, C. L., Sakulyanontvittaya, T., Duhl, T., Emmons, L. K., and Wang, X.:

908 The model of emissions of gases and aerosols from nature version 2.1 (MEGAN2.1): an extended and
 909 updated framework for modeling biogenic emissions, *Geosci. Model. Dev.*, 5, 1471-1492,
 910 10.5194/gmd-5-1471-2012, 2012.

911 Haque, M. M., Kawamura, K., and Kim, Y.: Seasonal variations of biogenic secondary organic aerosol
 912 tracers in ambient aerosols from Alaska, *Atmos. Environ.*, 130, 95-104,
 913 10.1016/j.atmosenv.2015.09.075, 2016.

914 He, M., Zheng, J., Yin, S., and Zhang, Y.: Trends, temporal and spatial characteristics, and uncertainties
 915 in biomass burning emissions in the Pearl River Delta, China, *Atmos. Environ.*, 45, 4051-4059,
 916 10.1016/j.atmosenv.2011.04.016, 2011.

917 [He, Q. F., Ding, X., Wang, X. M., Yu, J. Z., Fu, X. X., Liu, T. Y., Zhang, Z., Xue, J., Chen, D. H., Zhong,](#)
 918 [L. J., and Donahue, N. M.: Organosulfates from pinene and isoprene over the Pearl River Delta, South](#)
 919 [China: Seasonal variation and implication in formation mechanisms, *Environ. Sci. Technol.*, 48, 9236-](#)
 920 [9245, 10.1021/es501299v, 2014.](#)

921 He, Q. F., Ding, X., Fu, X. X., Zhang, Y. Q., Wang, J. Q., Liu, Y. X., Tang, M. J., Wang, X. M., and
 922 Rudich, Y.: Secondary organic aerosol formation from isoprene epoxides in the Pearl River Delta,
 923 South China: IEPOX- and HMML- derived tracers, *J. Geophys. Res.-Atmos.*, 123, 6999-7012,
 924 10.1029/2017JD028242, 2018.

925 Hofzumahaus, A., Rohrer, F., Lu, K., Bohn, B., Brauers, T., Chang, C.-C., Fuchs, H., Holland, F., Kita,
 926 K., Kondo, Y., Li, X., Lou, S., Shao, M., Zeng, L., Wahner, A., and Zhang, Y.: Amplified trace gas
 927 removal in the troposphere, *Science*, 324, 1702-1704, 10.1126/science.1164566, 2009.

928 Hoyle, C. R., Boy, M., Donahue, N. M., Fry, J. L., Glasius, M., Guenther, A., Hallar, A. G., Huff Hartz,
 929 K., Petters, M. D., Petäjä, T., Rosenoern, T., and Sullivan, A. P.: A review of the anthropogenic
 930 influence on biogenic secondary organic aerosol, *Atmos. Chem. Phys.*, 11, 321-343, 10.5194/acp-11-
 931 321-2011, 2011.

932 Hu, Q. H., Xie, Z. Q., Wang, X. M., Kang, H., He, Q. F., and Zhang, P.: Secondary organic aerosols over
 933 oceans via oxidation of isoprene and monoterpenes from Arctic to Antarctic, *Sci. Rep.*, 3, 2280,
 934 10.1038/srep02280, 2013.

935 [Jaoui, M., Lewandowski, M., Kleindienst, T. E., Offenberg, J. H., and Edney, E. O.: \$\beta\$ -caryophyllinic](#)
 936 [acid: An atmospheric tracer for \$\beta\$ -caryophyllene secondary organic aerosol, *Geophys. Res. Lett.*, 34,](#)
 937 [10.1029/2006gl028827, 2007.](#)

删除的内容: -

删除的内容: -

删除的内容: .

- 940 Keeling, C. I., and Bohlmann, J.: Genes, enzymes and chemicals of terpenoid diversity in the constitutive
941 and induced defence of conifers against insects and pathogens, *New Phytol.*, 170, 657-675,
942 10.1111/j.1469-8137.2006.01716.x, 2006.
- 943 Kleindienst, T. E., Jaoui, M., Lewandowski, M., Offenberg, J. H., Lewis, C. W., Bhawe, P. V., and Edney,
944 E. O.: Estimates of the contributions of biogenic and anthropogenic hydrocarbons to secondary organic
945 aerosol at a southeastern US location, *Atmos. Environ.*, 41, 8288-8300,
946 10.1016/j.atmosenv.2007.06.045, 2007.
- 947 [Lai, C., Liu, Y., Ma, J., Ma, Q., Chu, B., and He, H.: Heterogeneous kinetics of cis-pinonic acid with](#)
948 [hydroxyl radical under different environmental conditions, *J. Phys. Chem. A.*, 119, 6583-6593,](#)
949 [10.1021/acs.jpca.5b01321, 2015.](#)
- 950 Lewandowski, M., Piletic, I. R., Kleindienst, T. E., Offenberg, J. H., Beaver, M. R., Jaoui, M., Docherty,
951 K. S., and Edney, E. O.: Secondary organic aerosol characterisation at field sites across the United
952 States during the spring–summer period, *Int. J. Environ. An. Ch.*, 93, 1084-1103,
953 10.1080/03067319.2013.803545, 2013.
- 954 Li, J., Wang, G., Wu, C., Cao, C., Ren, Y., Wang, J., Li, J., Cao, J., Zeng, L., and Zhu, T.: Characterization
955 of isoprene-derived secondary organic aerosols at a rural site in North China Plain with implications
956 for anthropogenic pollution effects, *Sci. Rep.*, 8, 535, 10.1038/s41598-017-18983-7, 2018.
- 957 Lin, Y.-H., Zhang, Z., Docherty, K. S., Zhang, H., Budisulistiorini, S. H., Rubitschun, C. L., Shaw, S.,
958 Knipping, E., Edgerton, E. S., Kleindienst, T. E., Gold, A., and Surratt, J. D.: Isoprene epoxydiols as
959 precursors to secondary organic aerosol formation: Acid-catalyzed reactive uptake studies with
960 authentic standards, *Environ. Sci. Technol.*, 46, 189-195, 10.1021/es202554e, 2012.
- 961 Lopez-Hilfiker, F. D., Mohr, C., D'Ambro, E. L., Lutz, A., Riedel, T. P., Gaston, C. J., Iyer, S., Zhang,
962 Z., Gold, A., Surratt, J. D., Lee, B. H., Kurten, T., Hu, W. W., Jimenez, J., Hallquist, M., and Thornton,
963 J. A.: Molecular composition and volatility of organic aerosol in the southeastern U.S.: Implications
964 for IEPOX derived SOA, *Environ. Sci. Technol.*, 50, 2200-2209, 10.1021/acs.est.5b04769, 2016.
- 965 Lu, Q., Zheng, J., Ye, S., Shen, X., Yuan, Z., and Yin, S.: Emission trends and source characteristics of
966 SO₂, NO_x, PM₁₀ and VOCs in the Pearl River Delta region from 2000 to 2009, *Atmos. Environ.*, 76,
967 11-20, 10.1016/j.atmosenv.2012.10.062, 2013.
- 968 Müller, L., Reinnig, M. C., Naumann, K. H., Saathoff, H., Mentel, T. F., Donahue, N. M., and Hoffmann,
969 T.: Formation of 3-methyl-1,2,3-butanetricarboxylic acid via gas phase oxidation of pinonic acid – a

971 mass spectrometric study of SOA aging, *Atmos. Chem. Phys.*, 12, 1483-1496, 10.5194/acp-12-1483-
 972 2012, 2012.

973 Mentel, T. F., Kleist, E., Andres, S., Maso, M. D., Hohaus, T., Kiendler-Scharr, A., Rudich, Y., Springer,
 974 M., Tillmann, R., Uerlings, R., Wahner, A., and Wildt, J.: Secondary aerosol formation from stress-
 975 induced biogenic emissions and possible climate feedbacks, *Atmos. Chem. Phys.*, 13, 8755-8770,
 976 10.5194/acp-13-8755-2013, 2013.

977 Nguyen, T. B., Bates, K. H., Crounse, J. D., Schwantes, R. H., Zhang, X., Kjaergaard, H. G., Surratt, J.
 978 D., Lin, P., Laskin, A., Seinfeld, J. H., and Wennberg, P. O.: Mechanism of the hydroxyl radical
 979 oxidation of methacryloyl peroxyxynitrate (MPAN) and its pathway toward secondary organic aerosol
 980 formation in the atmosphere, *Phys. Chem. Chem. Phys.*, 17, 17914-17926, 10.1039/C5CP02001H,
 981 2015.

982 Offenberg, J. H., Lewis, C. W., Lewandowski, M., Jaoui, M., Kleindienst, T. E., and Edney, E. O.:
 983 Contributions of toluene and α -pinene to SOA formed in an irradiated toluene/ α -pinene/ NO_x /air
 984 mixture: Comparison of results using ^{14}C content and SOA organic tracer methods, *Environ. Sci.*
 985 *Technol.*, 41, 3972-3976, 10.1021/es070089+, 2007.

986 Offenberg, J. H., Lewandowski, M., Edney, E. O., Kleindienst, T. E., and Jaoui, M.: Influence of aerosol
 987 acidity on the formation of secondary organic aerosol from biogenic precursor hydrocarbons, *Environ.*
 988 *Sci. Technol.*, 43, 7742-7747, 10.1021/es901538e, 2009.

989 Ou, J., Yuan, Z., Zheng, J., Huang, Z., Shao, M., Li, Z., Huang, X., Guo, H., and Louie, P. K. K.: Ambient
 990 ozone control in a photochemically active region: Short-term despiking or long-term attainment?,
 991 *Environ. Sci. Technol.*, 50, 5720-5728, 10.1021/acs.est.6b00345, 2016.

992 Paulot, F., Crounse, J. D., Kjaergaard, H. G., Kürten, A., St. Clair, J. M., Seinfeld, J. H., and Wennberg,
 993 P. O.: Unexpected epoxide formation in the gas-phase photooxidation of isoprene, *Science*, 325, 730-
 994 733, 10.1126/science.1172910, 2009.

995 Pye, H. O. T., Pinder, R. W., Piletic, I. R., Xie, Y., Capps, S. L., Lin, Y.-H., Surratt, J. D., Zhang, Z., Gold,
 996 A., Luecken, D. J., Hutzell, W. T., Jaoui, M., Offenberg, J. H., Kleindienst, T. E., Lewandowski, M.,
 997 and Edney, E. O.: Epoxide pathways improve model predictions of isoprene markers and reveal key
 998 role of acidity in aerosol formation, *Environ. Sci. Technol.*, 47, 11056-11064, 10.1021/es402106h,
 999 2013.

1000 Riva, M., Budisulistiorini, S. H., Zhang, Z., Gold, A., and Surratt, J. D.: Chemical characterization of

删除的内容:

secondary organic aerosol constituents from isoprene ozonolysis in the presence of acidic aerosol, Atmos. Environ., 130, 5-13, 10.1016/j.atmosenv.2015.06.027, 2016.

Riva, M., Budisulistiorini, S. H., Zhang, Z., Gold, A., Thornton, J. A., Turpin, B. J., and Surratt, J. D.: Multiphase reactivity of gaseous hydroperoxide oligomers produced from isoprene ozonolysis in the presence of acidified aerosols, Atmos. Environ., 152, 314-322, 10.1016/j.atmosenv.2016.12.040, 2017.

Shen, R. Q., Ding, X., He, Q. F., Cong, Z. Y., Yu, Q. Q., and Wang, X. M.: Seasonal variation of secondary organic aerosol tracers in Central Tibetan Plateau, Atmos. Chem. Phys., 15, 8781-8793, 10.5194/acp-15-8781-2015, 2015.

Sipilä, M., Jokinen, T., Berndt, T., Richters, S., Makkonen, R., Donahue, N. M., Mauldin III, R. L., Kurtén, T., Paasonen, P., Sarnela, N., Ehn, M., Junninen, H., Rissanen, M. P., Thornton, J., Stratmann, F., Herrmann, H., Worsnop, D. R., Kulmala, M., Kerminen, V. M., and Petäjä, T.: Reactivity of stabilized Criegee intermediates (sCIs) from isoprene and monoterpene ozonolysis toward SO₂ and organic acids, Atmos. Chem. Phys., 14, 12143-12153, 10.5194/acp-14-12143-2014, 2014.

St. Clair, J. M., Rivera-Rios, J. C., Crounse, J. D., Knap, H. C., Bates, K. H., Teng, A. P., Jørgensen, S., Kjaergaard, H. G., Keutsch, F. N., and Wennberg, P. O.: Kinetics and products of the reaction of the first-generation isoprene hydroxy hydroperoxide (ISOPOOH) with OH, J. Phys. Chem. A., 120, 1441-1451, 10.1021/acs.jpca.5b06532, 2016.

Stone, E. A., Nguyen, T. T., Pradhan, B. B., and Man Dangol, P.: Assessment of biogenic secondary organic aerosol in the Himalayas, Environ. Chem., 9, 263-272, 10.1071/EN12002, 2012.

Surratt, J. D., Chan, A. W. H., Eddingsaas, N. C., Chan, M., Loza, C. L., Kwan, A. J., Hersey, S. P., Flagan, R. C., Wennberg, P. O., and Seinfeld, J. H.: Reactive intermediates revealed in secondary organic aerosol formation from isoprene, P. Natl. Acad. Sci. USA., 107, 6640-6645, 10.1073/P.Natl.Acad.Sci.USA.0911114107, 2010.

[Szmigielski, R., Surratt, J. D., Gómez-González, Y., Van der Veken, P., Kourtev, I., Vermeylen, R., Blockhuys, F., Jaoui, M., Kleindienst, T. E., Lewandowski, M., Offenberg, J. H., Edney, E. O., Seinfeld, J. H., Maenhaut, W., and Claeys, M.: 3-methyl-1,2,3-butanetricarboxylic acid: An atmospheric tracer for terpene secondary organic aerosol, Geophys. Res. Lett., 34, 10.1029/2007gl031338, 2007.](#)

Von Schneidemesser, E., Monks, P. S., Allan, J. D., Bruhwiler, L., Forster, P., Fowler, D., Lauer, A., Morgan, W. T., Paasonen, P., Righi, M., Sindelarova, K., and Sutton, M. A.: Chemistry and the linkages between air quality and climate change, Chem. Rev., 115, 3856-3897, 10.1021/acs.chemrev.5b00089, 2015.

2015.

[Wang, W., Kourtchev, I., Graham, B., Cafmeyer, J., Maenhaut, i., and Claeys, M.: Characterization of oxygenated derivatives of isoprene related to 2-methyltetrols in Amazonian aerosols using trimethylsilylation and gas chromatography/ion trap mass spectrometry, *Rapid Commun. Mass Spectrom.*, **19**, 1343-1351, 10.1002/rcm.1940, 2005.](#)

Wang, X., Liu, H., Pang, J., Carmichael, G., He, K., Fan, Q., Zhong, L., Wu, Z., and Zhang, J.: Reductions in sulfur pollution in the Pearl River Delta region, China: Assessing the effectiveness of emission controls, *Atmos. Environ.*, **76**, 113-124, 10.1016/j.atmosenv.2013.04.074, 2013.

[Watanabe, A. C., Stropoli, S. J., and Elrod, M. J.: Assessing the potential mechanisms of isomerization reactions of isoprene epoxydiols on secondary organic aerosol, *Environ. Sci. Technol.*, **52**, 8346-8354, 10.1021/acs.est.8b01780, 2018.](#)

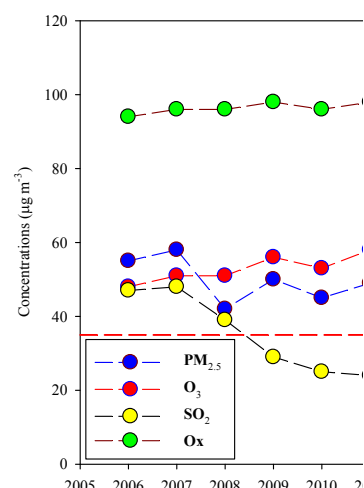
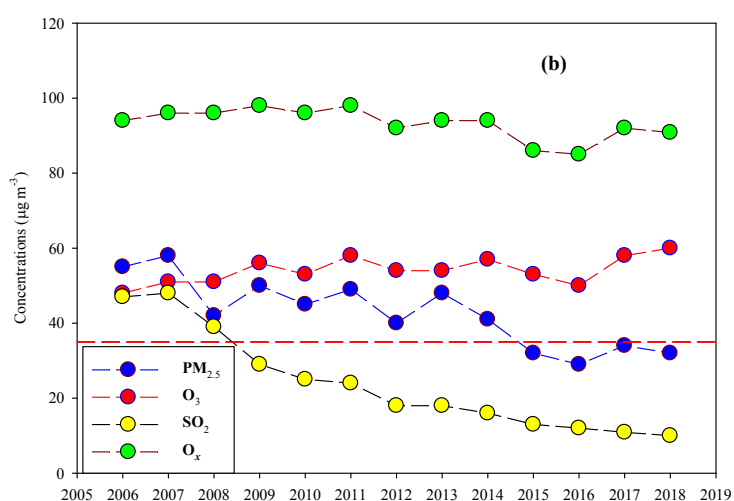
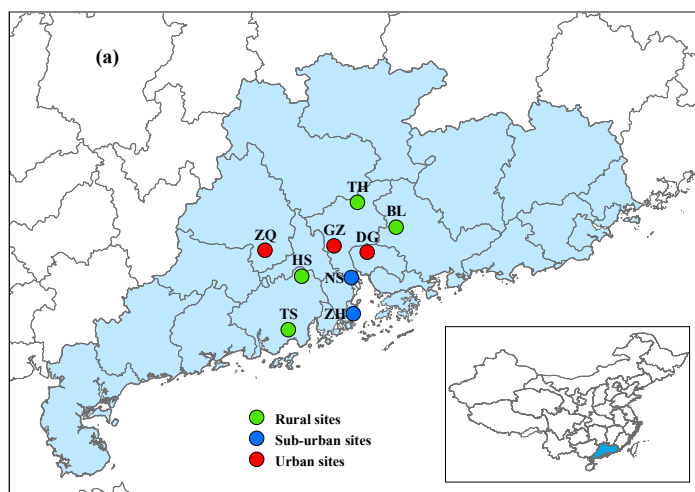
Worton, D. R., Surratt, J. D., LaFranchi, B. W., Chan, A. W. H., Zhao, Y., Weber, R. J., Park, J.-H., Gilman, J. B., de Gouw, J., Park, C., Schade, G., Beaver, M., Clair, J. M. S., Crounse, J., Wennberg, P., Wolfe, G. M., Harrold, S., Thornton, J. A., Farmer, D. K., Docherty, K. S., Cubison, M. J., Jimenez, J.-L., Frossard, A. A., Russell, L. M., Kristensen, K., Glasius, M., Mao, J., Ren, X., Brune, W., Browne, E. C., Pusede, S. E., Cohen, R. C., Seinfeld, J. H., and Goldstein, A. H.: Observational insights into aerosol formation from isoprene, *Environ. Sci. Technol.*, **47**, 11396–11402, 10.1021/es4011064, 2013.

Xu, L., Guo, H., Boyd, C. M., Klein, M., Bougiatioti, A., Cerully, K. M., Hite, J. R., Isaacman-VanWertz, G., Kreisberg, N. M., Knote, C., Olson, K., Koss, A., Goldstein, A. H., Hering, S. V., de Gouw, J., Baumann, K., Lee, S.-H., Nenes, A., Weber, R. J., and Ng, N. L.: Effects of anthropogenic emissions on aerosol formation from isoprene and monoterpenes in the southeastern United States, *P. Natl. Acad. Sci. USA.*, **112**, 37-42, 10.1073/P.Natl.Acad.Sci.USA.1417609112, 2015.

Xu, L., Middlebrook, A. M., Liao, J., de Gouw, J. A., Guo, H., Weber, R. J., Nenes, A., Lopez-Hilfiker, F. D., Lee, B. H., Thornton, J. A., Brock, C. A., Neuman, J. A., Nowak, J. B., Pollack, I. B., Welti, A., Graus, M., Warneke, C., and Ng, N. L.: Enhanced formation of isoprene-derived organic aerosol in sulfur-rich power plant plumes during Southeast Nexus, *J. Geophys. Res-Atmos.*, **121**, 11137-11153, 10.1002/2016JD025156, 2016.

[Ye, J., Abbatt, J. P. D., and Chan, A. W. H.: Novel pathway of SO₂ oxidation in the atmosphere: Reactions with monoterpene ozonolysis intermediates and secondary organic aerosol, *Atmos. Chem. Phys.*, **18**, 5549-5565, 10.5194/acp-18-5549-2018, 2018.](#)

1062 Zhang, R. Y., Wang, G. H., Guo, S., Zarnora, M. L., Ying, Q., Lin, Y., Wang, W. G., Hu, M., and Wang,
1063 Y.: Formation of urban fine particulate matter, *Chem. Rev.*, 115, 3803-3855,
1064 10.1021/acs.chemrev.5b00067, 2015.
1065 Zheng, J., Zheng, Z., Yu, Y., and Zhong, L.: Temporal, spatial characteristics and uncertainty of biogenic
1066 VOC emissions in the Pearl River Delta region, China, *Atmos. Environ.*, 44, 1960-1969,
1067 10.1016/j.atmosenv.2010.03.001, 2010.
1068



删除的内容:

Figure 1 Sampling sites in the PRD (a) and long-term trends of annual-mean PM_{2.5}, O₃, SO₂ and O_x recorded by the Guangdong-Hong Kong-Macao regional air quality monitoring network (<http://www.gdep.gov.cn/hjjce/>) (b). The red dash line indicates the NAAQS for annual-mean PM_{2.5} concentrations (35 µg m⁻³).

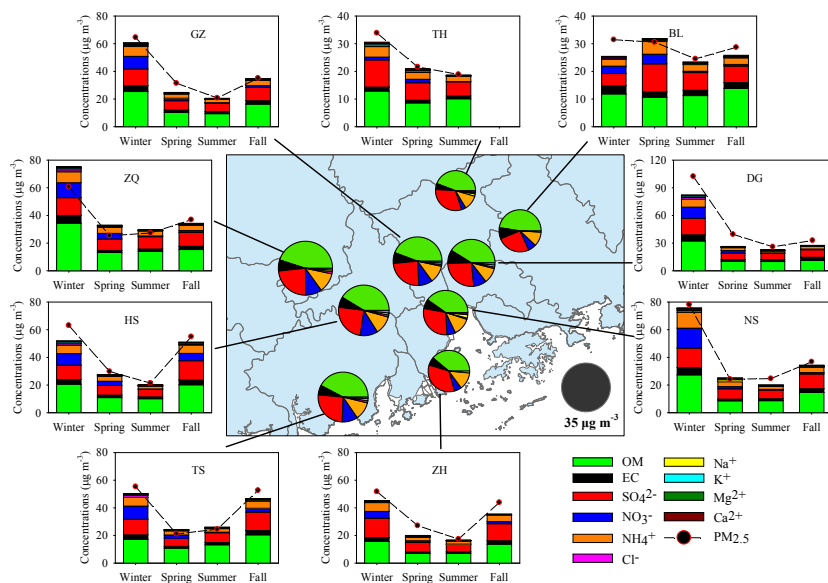


Figure 2 Major components in $PM_{2.5}$ and their seasonal variation at 9 sites. The pie charts in the central figure represent the annual average of major components. High levels of $PM_{2.5}$ and major components were observed in wintertime.

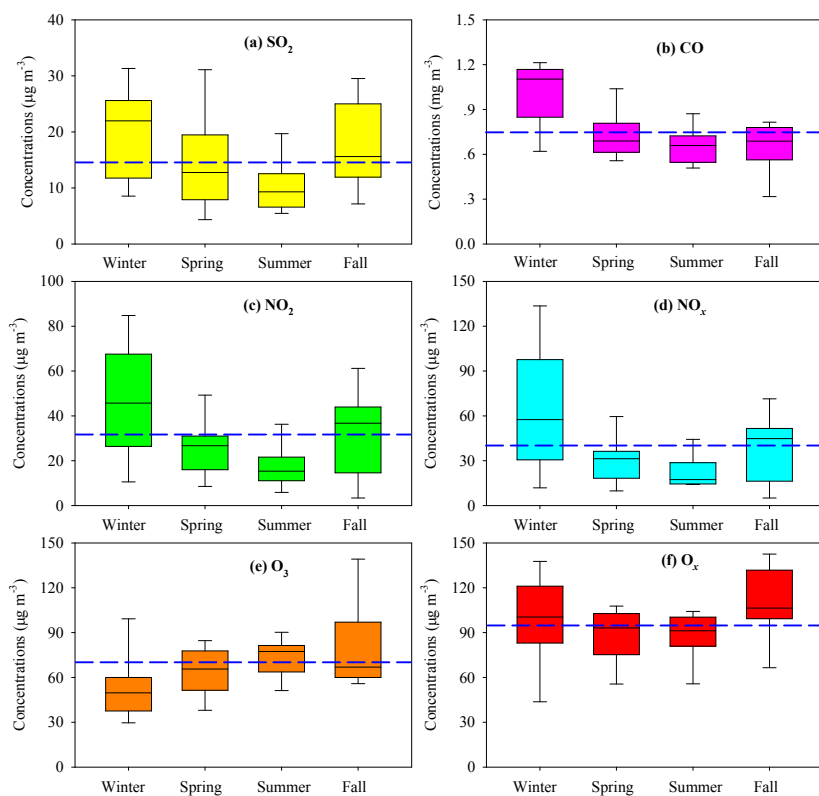
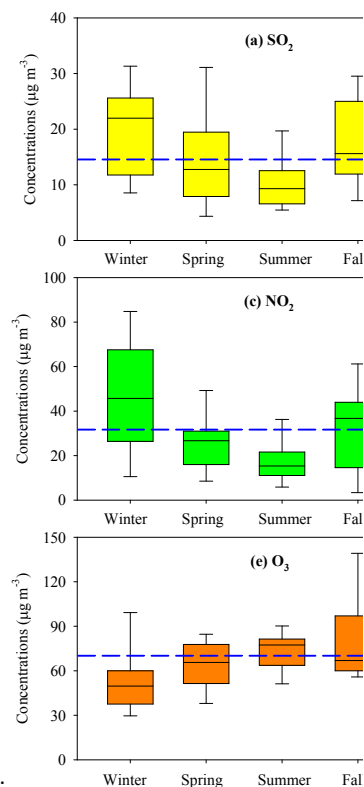


Figure 3 Seasonal variation of gaseous pollutants in the PRD. Box with error bars represent 10th, 25th, 75th, 90th percentiles for each pollutant. The line in each box represents the median value. Blue dash lines indicate annual average concentrations of SO₂ (14.9 $\mu\text{g m}^{-3}$), CO (0.74 mg m^{-3}), NO₂ (28.5 $\mu\text{g m}^{-3}$), NO_x (39.0 $\mu\text{g m}^{-3}$), O₃ (67.7 $\mu\text{g m}^{-3}$) and O_{3x} (96.1 $\mu\text{g m}^{-3}$).

删除的内容:



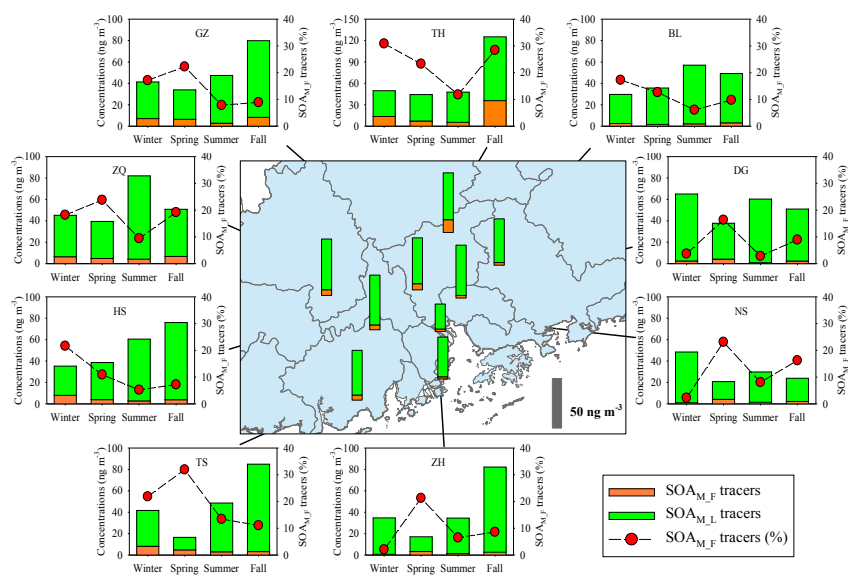
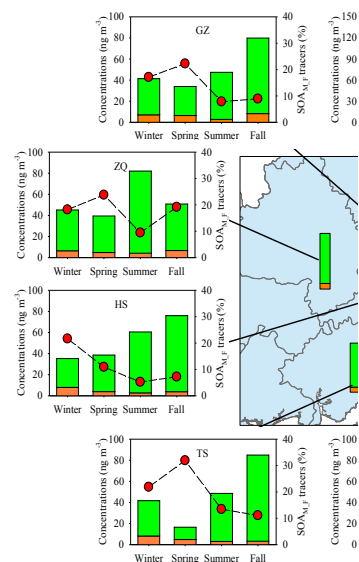


Figure 4 Spatial and seasonal variations of SOA_M tracers at 9 sites in the PRD. The bars in the central figure represent the annual average concentrations of the SOA_M tracers.

删除的内容:



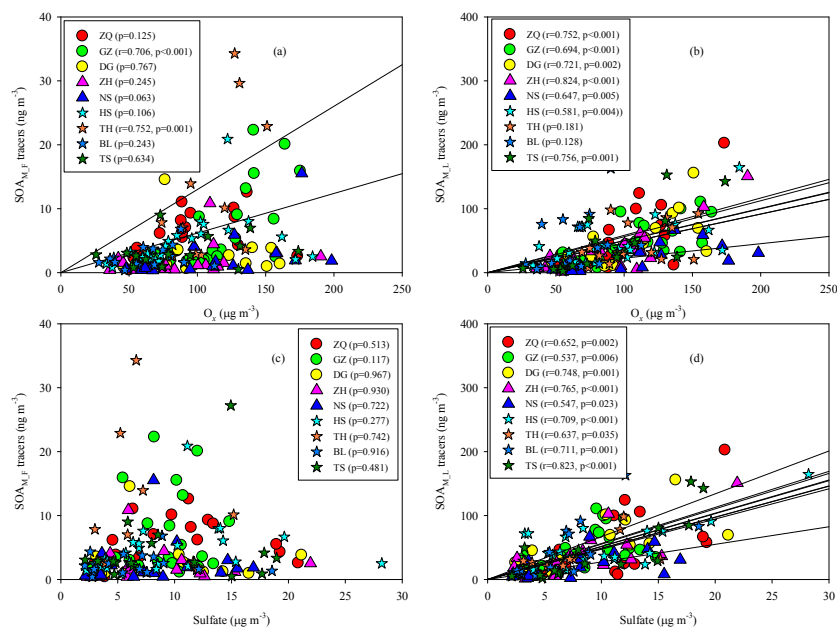
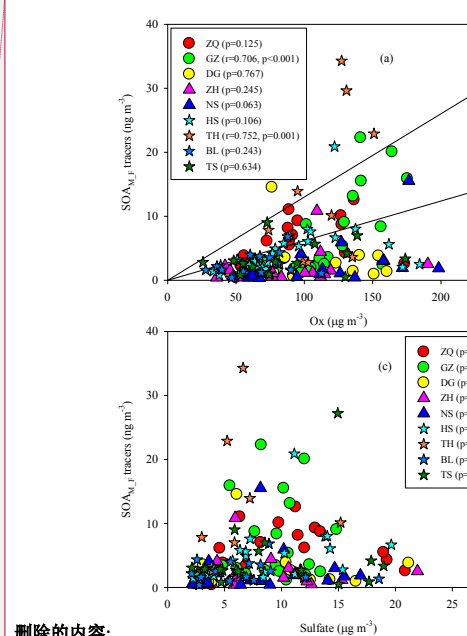


Figure 5 Correlations of SOA_{M_F} and SOA_{M_L} tracers with O₃ (a, b) and sulfate (c, d)



删除的内容:

删除的内容: H

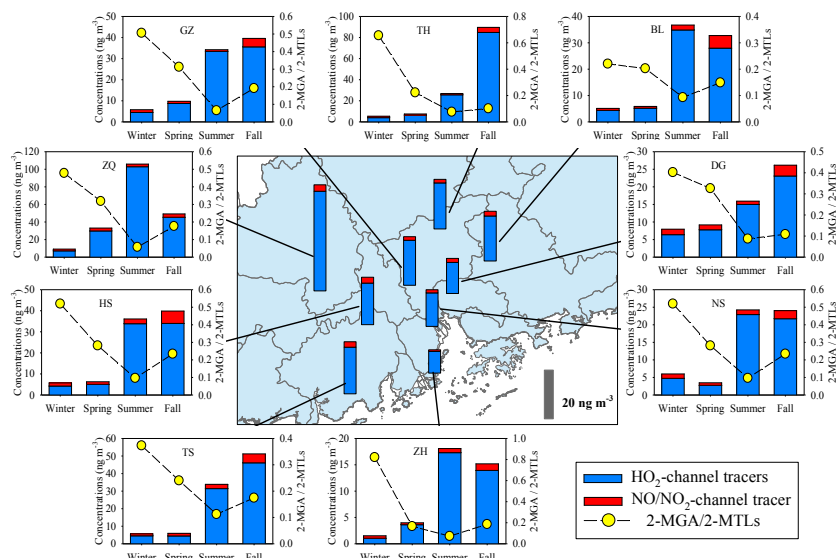


Figure 6 Spatial and seasonal variations of SOA₁ tracers at 9 sites in the PRD. The bars in the central figure represent the annual average concentrations of the SOA₁ tracers.

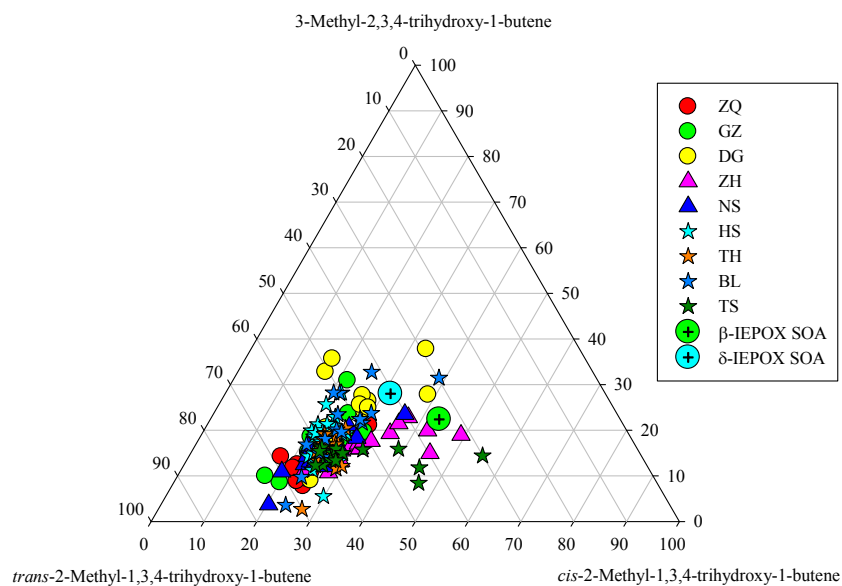


Figure 7 Ternary plot of C₅-alkene triol isomers in the PRD samples and in the β-IEPOX and δ-IEPOX derived SOA (Lin et al., 2012).

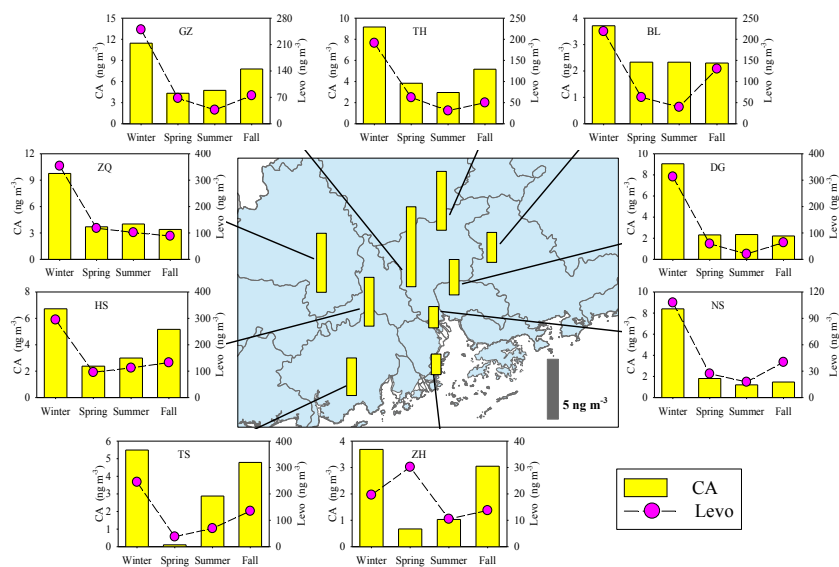


Figure 8 Spatial and seasonal variations of SOA_c tracer (CA) at 9 sites in the PRD. The bars in the central figure represent the annual average concentration of the SOA_c tracers. The pink circle indicates the BB tracer, levoglucosan (Levo).

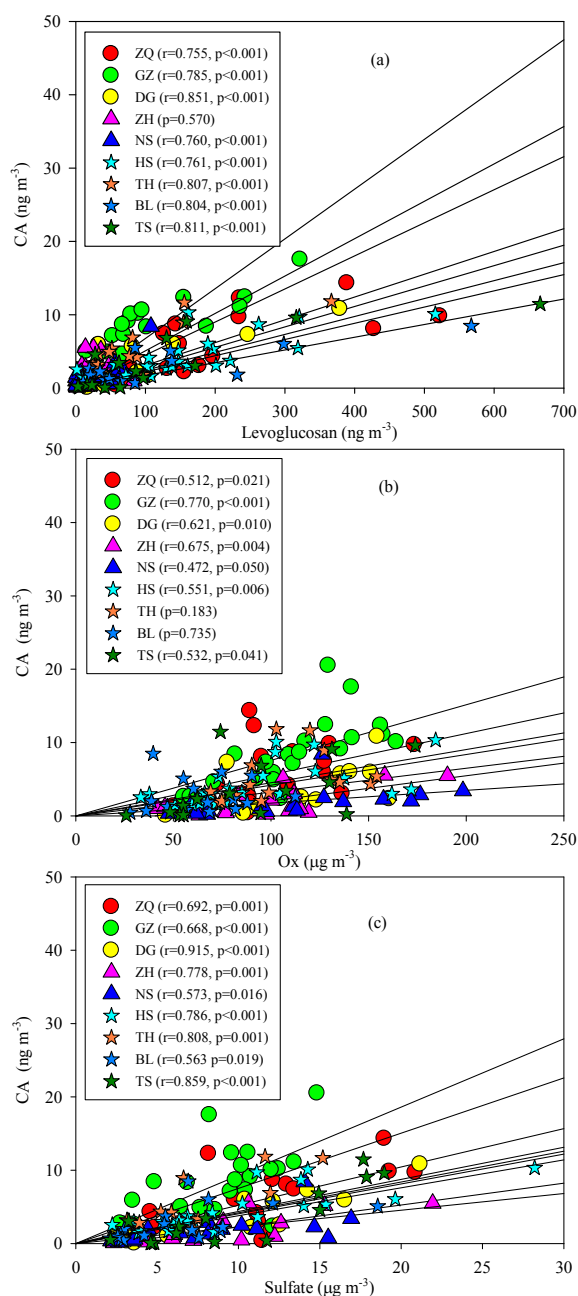


Figure 9 Significant correlations of CA with levoglucosan (a), O_x (b) and sulfate (c).

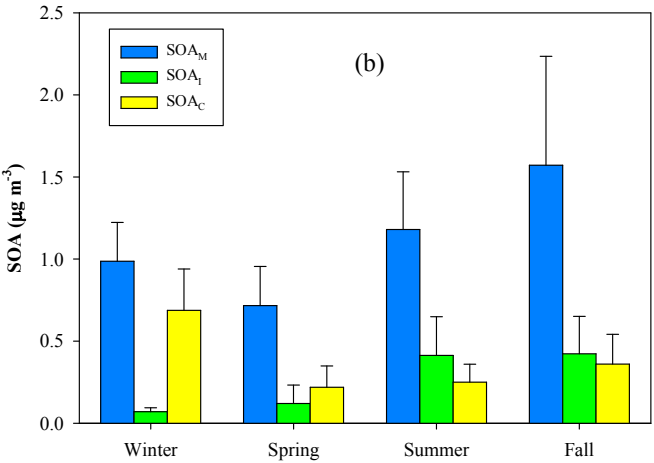
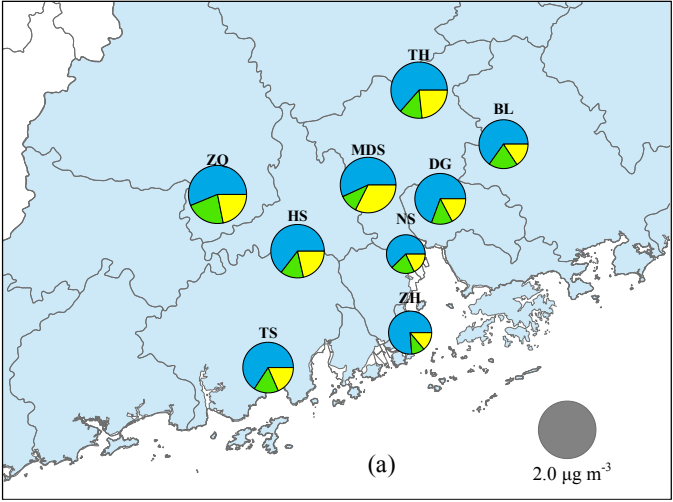


Figure 10 Spatial (a) and seasonal variations (b) of BSOA

1120 Table 1 Correlations between SOA_I tracers and NO_x

	2-MGA		2-MGA/2-MTLs	
	Coefficient (r)	<i>p</i> -value	Coefficient (r)	<i>p</i> -value
NO	0.028	0.733	0.166	0.043
NO ₂	0.205	0.008	0.352	<0.001
NO _x	0.132	0.102	0.286	<0.001
NO ₂ /NO	0.001	0.986	0.162	0.048

1121

1122

1123 Table 2 Correlations of BSOA with sulfate and O_x

	Sulfate			O _x		
	Slope	<i>p</i> -value	% ^a	Slope	<i>p</i> -value	% ^a
SOA _M	0.112	<0.001	45	0.013	<0.001	57
SOA _I	0.020	<0.001	34	0.003	<0.001	50
SOA _C	0.041	<0.001	46	0.004	<0.001	55
BSOA	0.172	<0.001	44	0.019	<0.001	55

1124 ^a Percentages of SOA reduction at 50% decline of sulfate or O_x

1125

Supporting Information

Impact of anthropogenic emissions on biogenic secondary organic aerosol: Observation in the Pearl River Delta, South China

Yu-Qing Zhang^{1, *}, Duo-Hong Chen^{2, *}, Xiang Ding^{1, †}, Jun Li¹, Tao Zhang², Jun-Qi Wang¹, Qian Cheng^{1, 3}, Hao Jiang¹, Wei Song¹, Yu-Bo Ou², Peng-Lin Ye³, Gan Zhang¹, Xin-Ming Wang^{1, 4}

- 1 State Key Laboratory of Organic Geochemistry and Guangdong Provincial Key Laboratory of Environmental Protection and Resources Utilization, Guangzhou Institute of Geochemistry, Chinese Academy of Sciences, Guangzhou, 510640, China
- 2 State Environmental Protection Key Laboratory of Regional Air Quality Monitoring, Environmental Monitoring Center of Guangdong Province, Guangzhou, 510308, China
- 3 Aerodyne Research Inc., Billerica, Massachusetts 01821, United States
- 4 Center for Excellence in Regional Atmospheric Environment, Institute of Urban Environment, Chinese Academy of Sciences, Xiamen, 361021, China

* These authors contributed equally to this work.
† Correspondence to: Xiang Ding (xiangd@gig.ac.cn)

Contents of this file

Text S1

Figure S1 to S10

Table S1 to S7

删除的内容: 6
删除的内容: 5

Text S1 SOA-tracer method for source apportionment

The SOA-tracer method is developed by Kleindienst and co-workers. Based on chamber experiments, they determine the mass fractions of tracers in SOA (f_{SOA}) and SOC (f_{SOC}) for individual precursor:

$$f_{\text{SOA}} = \frac{\sum [\text{tr}_i]}{[\text{SOA}]}, \quad f_{\text{SOC}} = \frac{\sum [\text{tr}_i]}{[\text{SOC}]}$$

where $\sum [\text{tr}_i]$ is the sum of tracer concentrations for a precursor, and [SOA] and [SOC] are the measured SOA and SOC concentrations in chamber-generated SOA samples. The available f_{SOA} and f_{SOC} values were listed in Table S2. With these mass fractions in literatures and measured SOA tracers in the ambient air, SOA and SOC from different precursors have been estimated in different places of the world (Hu et al., 2008; Lewandowski et al., 2013; Stone et al., 2012; von Schneidmesser et al., 2009; Ding et al., 2014), with the assumption that the f_{SOA} and f_{SOC} values in the chamber samples are the same in the ambient air. In this study, the same set of SOA tracers reported by Kleindienst and co-workers were used for the SOC and SOA estimations (Table S2).

The uncertainty in the SOA-tracer method is induced from the analysis of organic tracers and the determination of conversion factors. The uncertainties in the tracers' analyses were estimated in the range of 15-157% (Table S2). The uncertainties in f_{SOA} were reported to be 25% for isoprene, 48% for monoterpenes, and 22% for β -caryophyllene (Kleindienst et al., 2007; Lewandowski et al., 2013). Considering these factors, the uncertainty of the estimating procedure was calculated through error propagation. The relative standard deviations (RSD) were 37% for SOA_i , 67% for SOA_M , and 158% for SOA_C . On average, the RSD of total BSOA (sum of the three BVOCs) was 59%.

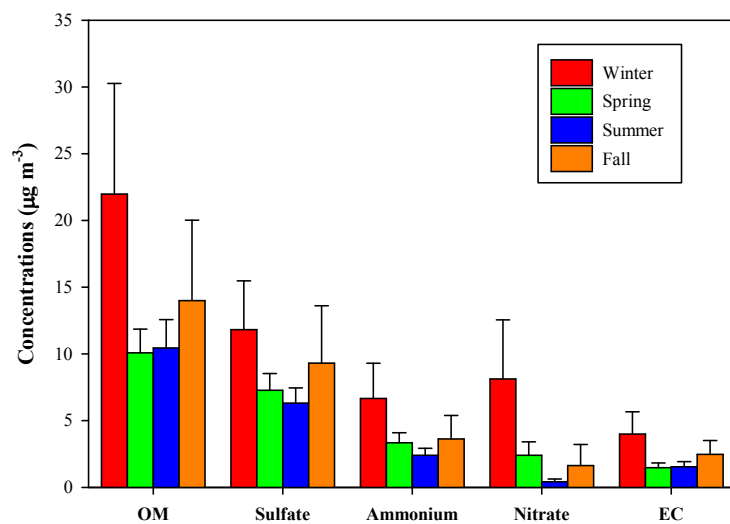


Figure S1 Seasonal variation of major components in PM_{2.5}. All the major components increased in winter and fall.

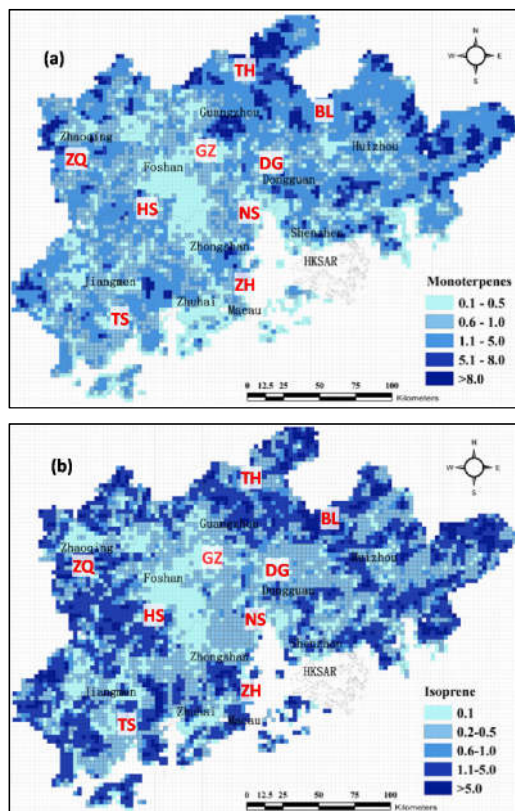


Figure S2 Spatial distribution of monoterpenes (a), and isoprene (b) emissions in the PRD (Zheng et al., 2010). The sampling sites are labeled.

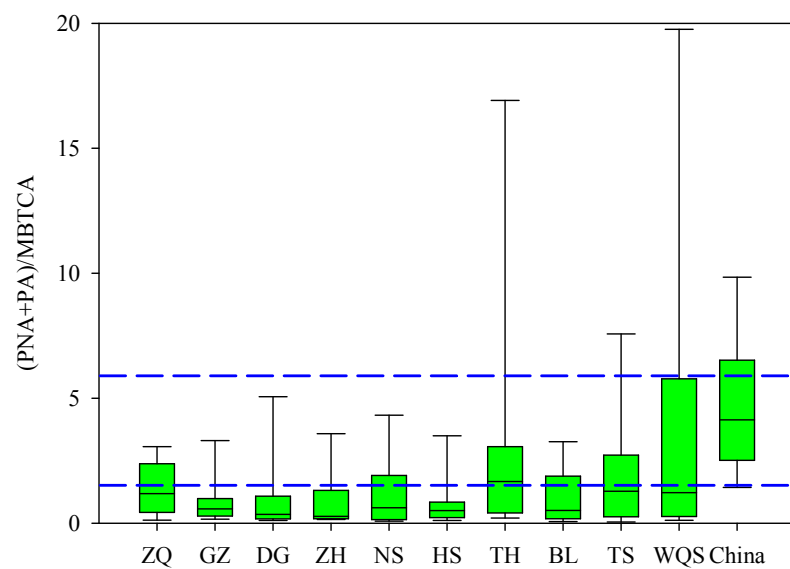


Figure S3 Spatial distribution of (PNA+PA)/MBTCA ratios at 9 sites in the PRD. The (PNA+PA)/MBTCA ratios between two blue dash lines (1.51–5.91) indicate fresh SOA_M from chamber studies (Eddingsaas et al., 2012; Offenberg et al., 2007). Box with error bars represent 10th, 25th, 75th, 90th percentiles at each site. The line in the box is the median at each site. The data at WQS site during 2008 in the PRD (Ding et al., 2012) and at 12 sites during 2012–2013 in China (Ding et al., 2016) were reported in our previous studies.

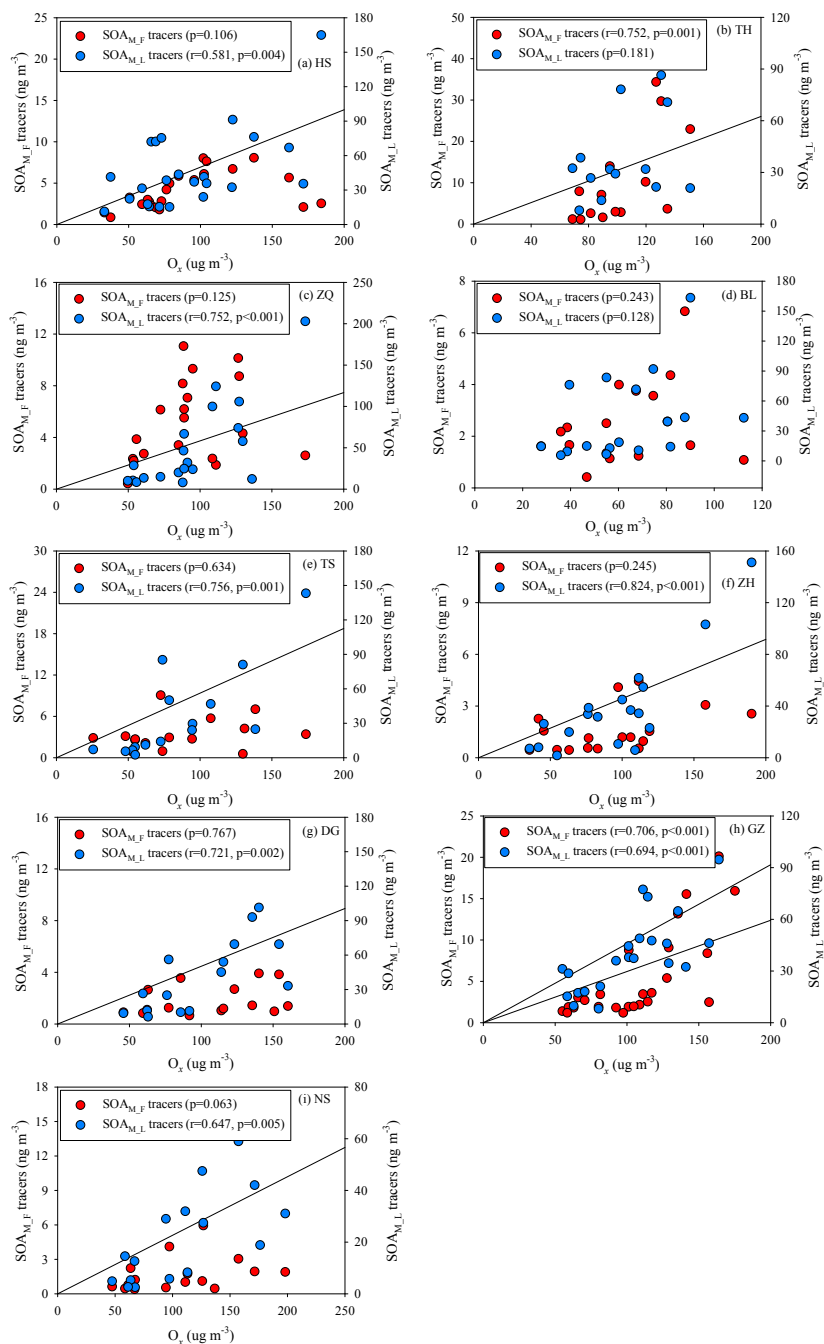


Figure S4 Correlations of SOA_{M,F} tracers and SOA_{M,L} tracers with O_x

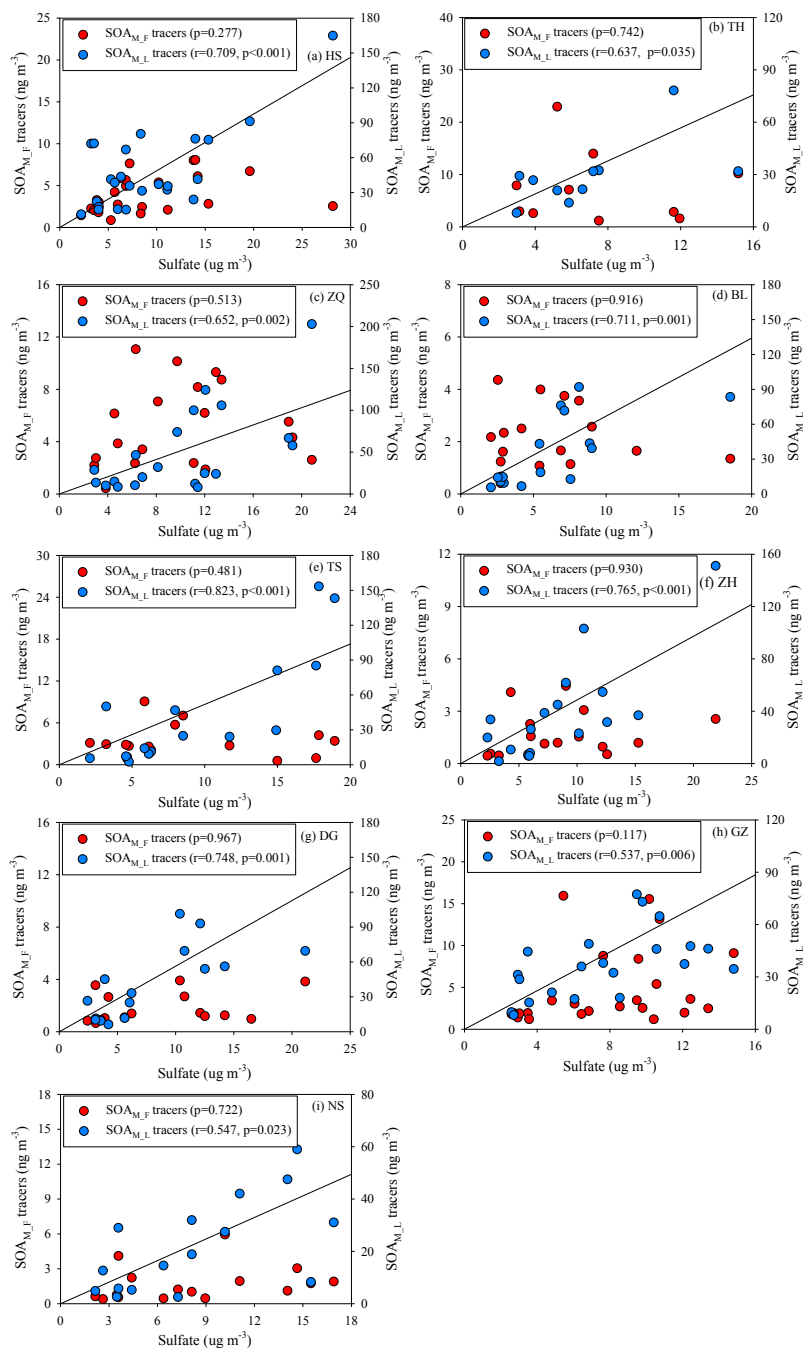


Figure S5 Correlations of $\text{SOA}_{M,F}$ tracers and $\text{SOA}_{M,L}$ tracers with sulfate

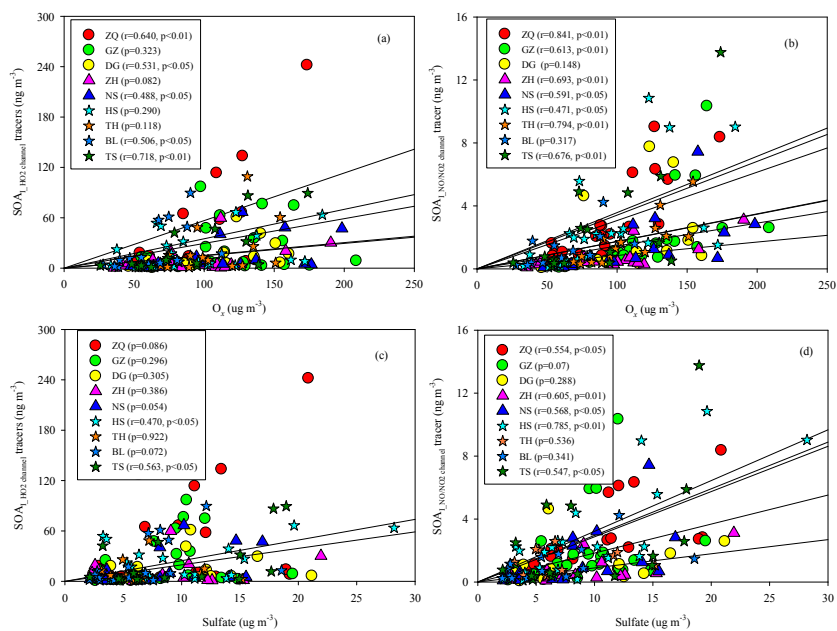


Figure S6 Correlations of SOA_{HO2-channel} tracers and SOA_{NO/NO2-channel} tracers with O_3 (a, b) and sulfate (c, d)

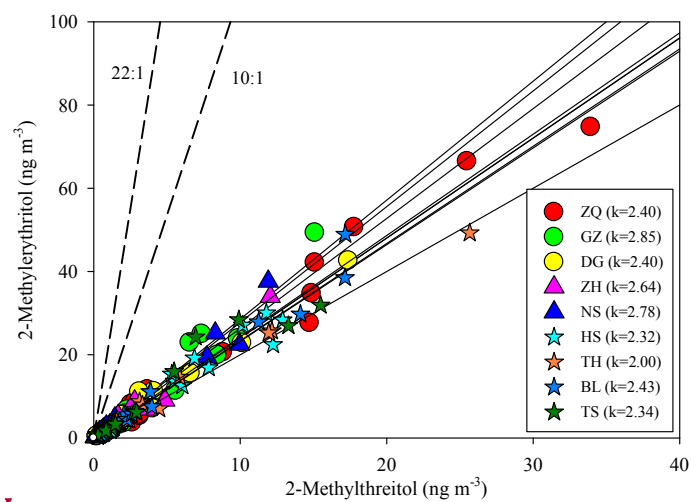


Figure S7. Significant correlations between 2-methyltetrol isomers at 9 sites in the PRD. K indicates the slope of each linear regression. The dash lines indicate the ratio range of 2-methyltetrol isomers in the SOA from isoprene ozonolysis (Riva et al., 2016).

删除的内容: 。

分页符

带格式的: 孤行控制

删除的内容: 4

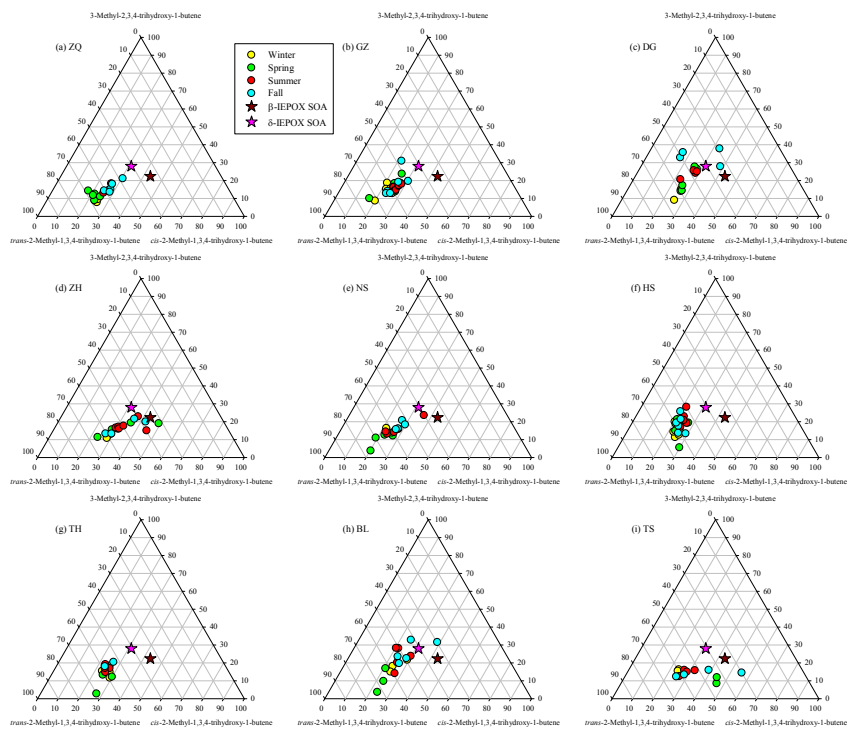


Figure S8 Intercomparison of C_5 -alkene triols compositions at 9 sites and in β -IEPOX and δ -IEPOX derived SOA (Lin et al., 2012).

删除的内容: 5

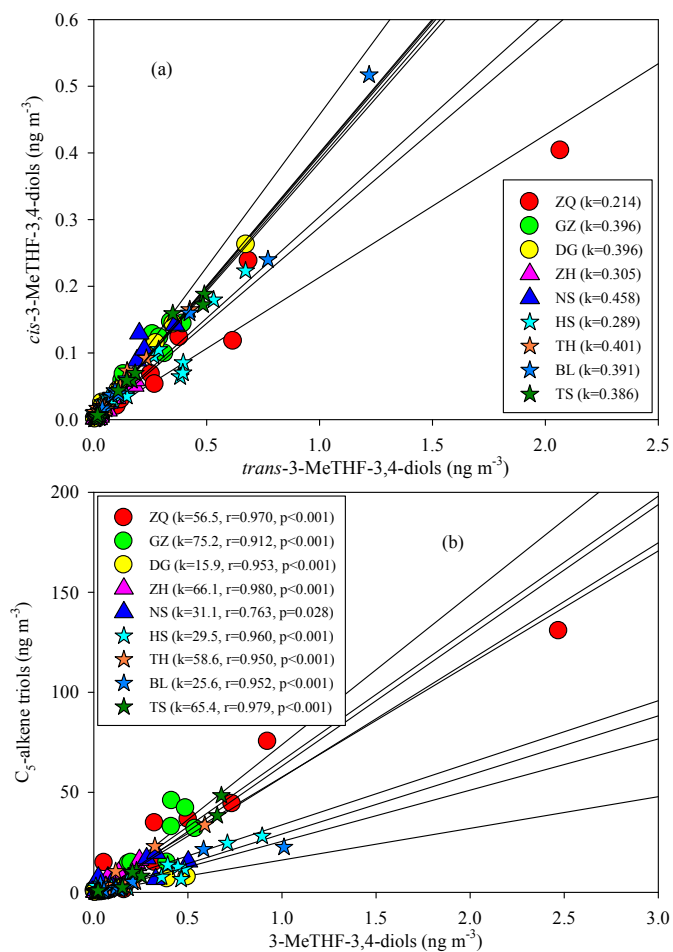


Figure S9. Significant correlations among the SOA₁ tracers. K indicates the slope of each linear regression.

删除的内容: 6

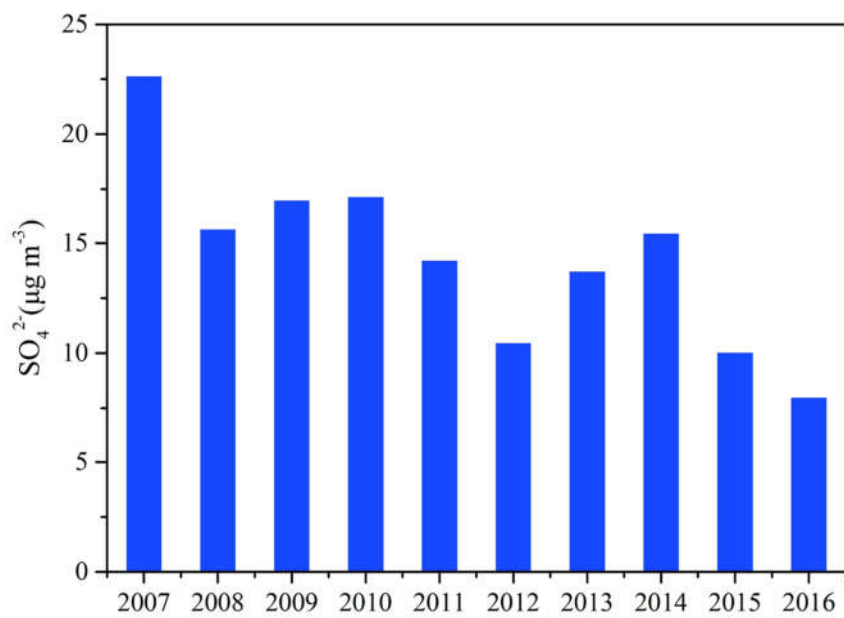


Figure S10 Long-term variation of sulfate in fall at WQS from 2007-2016.

带格式的：居中

Table S1 Data summary of gaseous and particulate species in the air of PRD

	Zhaoqing (ZQ, urban site)					Guangzhou (GZ, urban site)					Dongguan (DG, urban site)					Nansha (NS, sub-urban site)					Zhuhai (ZH, sub-urban site)				
	Winter	Spring	Summer	Fall	Annual	Winter	Spring	Summer	Fall	Annual	Winter	Spring	Summer	Fall	Annual	Winter	Spring	Summer	Fall	Annual	Winter	Spring	Summer	Fall	Annual
Temperature (°C)	15.1	22.8	29.1	24.2	22.7(12.8-31.3)	15.7	23.0	29.9	26.6	24.0(11.2-31.8)	18.1	23.0	30.3	25.3	24.9(15.9-32.0)	19.6	22.2	29.5	25.5	25.6(16.0-30.9)	16.6	22.5	29.5	24.4	24.2(14.7-31.1)
RH (%)	54	61	63	59	59(34-71)	52	59	64	55	58(26-83)	57	61	64	60	61(30-78)	72	67	68	63	67(33-82)	76	72	75	74	74(42-85)
SO ₂ (µg m ⁻³)	22.0	31.1	19.7	29.5	25.5(4.09-21.9)	23.4	15.7	7.38	15.4	15.1(3.43-41.3)	27.8	14.5	13.4	15.6	16.2(5.04-33.2)	22.9	12.8	9.30	20.5	14.4(4.04-36.5)	8.55	6.05	5.77	10.4	7.33(2.14-14.6)
NO ₂ (µg m ⁻³)	40.4	24.1	15.4	36.7	29.1(2.45-82.7)	84.8	49.3	36.3	61.2	57.2(29.7-155)	73.7	34.0	24.2	35.4	36.9(10.5-102)	61.4	27.6	19.0	44.4	31.4(8.08-91.7)	50.7	21.7	14.3	34.2	26.8(7.08-65.0)
NO (µg m ⁻³)	14.7	4.65	4.06	5.88	7.31(2.00-35.4)	31.8	6.73	5.24	6.65	12.7(1.13-126)	25.1	3.64	6.77	6.14	7.88(1.5-42.4)	13.5	2.48	2.00	6.16	4.04(0.56-13.5)	6.75	na	na	na	6.75(5.63-7.53)
NO _x (µg m ⁻³)	62.9	31.3	21.5	45.7	40.3(6.70-121)	134	59.5	44.3	71.4	76.8(35.2-349)	112	39.6	34.6	44.8	49.0(13.6-167)	83.0	32.1	22.7	54.4	38.3(10.3-111)	57.5	na	na	na	57.4(47.6-72.1)
O ₃ (µg m ⁻³)	55.2	64.3	81.9	59.6	65.2(11.8-145)	52.9	54.1	51.2	62.2	54.7(18.8-115)	42.3	65.6	80.0	66.9	66.6(31.5-123)	64.8	80.2	80.8	78.6	79.0(21.3-149)	49.7	48.7	66.3	106	67.5(18.3-155)
O ₃ (µg m ⁻³)	95.7	88.5	97.2	96.3	94.4(49.9-173)	138	103	87.5	123	112(55.3-208)	116	99.7	104	102	103(46.0-160)	126	108	99.8	123	110(47.7-198)	100	70.4	80.6	140	94.3(35.7-190)
CO (mg m ⁻³)	1.18	0.69	0.66	0.73	0.81(0.21-1.66)	1.21	1.04	0.73	0.78	0.94(0.52-1.81)	1.15	0.72	0.71	0.61	0.73(0.32-1.52)	0.85	0.74	0.66	0.69	0.70(0.37-1.21)	1.11	0.66	0.62	0.59	0.70(0.48-1.14)
OC (µgC m ⁻³)	21.5	8.26	8.73	9.60	12.0(4.66-32.1)	15.9	6.55	5.90	10.2	9.59(3.12-33.5)	20.2	6.51	6.28	7.09	8.34(3.46-27.7)	17.1	5.37	5.43	9.18	7.20(1.94-19.6)	9.82	4.41	4.50	8.55	6.05(1.94-17.5)
EC (µgC m ⁻³)	5.70	1.50	1.80	2.34	2.83(0.79-8.41)	4.35	1.58	1.60	2.51	2.51(0.79-11.7)	6.76	1.80	2.12	3.39	2.99(0.84-8.39)	5.32	1.22	1.48	2.71	1.99(0.44-6.61)	2.82	1.07	0.96	2.55	1.59(0.44-5.16)
SO ₄ ²⁻ (µg m ⁻³)	12.8	8.27	8.86	10.1	10.0(2.92-20.9)	12.0	6.72	5.78	9.55	8.44(2.61-19.5)	17.7	6.87	6.52	8.09	8.52(2.45-21.2)	14.1	7.48	6.18	10.6	8.32(2.18-16.9)	14.0	6.80	5.48	12.3	8.47(2.33-21.9)
NO ₃ ⁻ (µg m ⁻³)	10.8	4.05	0.54	1.31	4.18(0.14-21.5)	9.11	1.82	0.57	1.29	3.22(0.15-23.3)	12.3	2.92	0.75	0.79	2.88(0.23-16.2)	14.4	1.59	0.50	1.06	1.81(0.23-14.4)	4.97	1.28	0.16	1.53	1.38(0.04-5.91)
NH ₄ ⁺ (µg m ⁻³)	7.92	4.44	3.70	3.86	4.98(1.10-14.3)	7.10	2.98	2.26	3.87	4.03(0.95-12.8)	8.58	3.03	2.09	2.79	3.41(0.62-9.75)	11.5	3.54	2.33	3.91	3.69(0.93-11.5)	6.35	2.51	2.23	4.54	3.34(0.60-8.10)
Cl ⁻ (µg m ⁻³)	1.42	0.50	0.08	0.19	0.55(0.03-2.89)	0.86	0.37	0.13	0.14	0.37(0.06-1.78)	1.84	0.24	0.14	0.06	0.36(0.03-2.21)	1.33	0.44	0.09	0.20	0.30(0.04-1.44)	0.27	0.25	0.05	0.06	0.14(0.01-0.52)
Na ⁺ (µg m ⁻³)	0.83	0.34	0.29	0.36	0.45(0.08-2.66)	0.66	0.23	0.26	0.40	0.39(0.08-1.13)	0.73	0.38	0.51	0.38	0.46(0.11-0.96)	0.60	1.46	0.27	0.43	0.68(0.15-2.30)	0.48	0.46	0.28	0.34	0.37(0.09-0.71)
K ⁺ (µg m ⁻³)	0.83	0.38	0.23	0.33	0.44(0.11-1.32)	0.70	0.21	0.25	0.36	0.38(0.01-2.16)	1.45	0.36	0.20	0.35	0.45(0.14-1.95)	0.81	0.30	0.11	0.30	0.26(0.04-0.81)	0.46	0.22	0.09	0.24	0.21(0.02-0.58)
Mg ²⁺ (µg m ⁻³)	0.10	0.05	0.04	0.04	0.06(0.02-0.35)	0.08	0.04	0.03	0.04	0.05(0.01-0.18)	0.08	0.06	0.07	0.04	0.06(0.02-0.12)	0.07	0.15	0.11	0.08	0.11(0.03-0.21)	0.06	0.09	0.04	0.04	0.06(0.01-0.13)
Ca ²⁺ (µg m ⁻³)	0.59	0.31	0.37	0.44	0.44(0.07-1.14)	0.49	0.34	0.24	0.30	0.34(0.17-0.88)	0.42	0.32	0.32	0.30	0.33(0.11-0.79)	0.32	0.46	0.41	0.44	0.43(0.17-1.03)	0.22	0.29	0.07	0.17	0.18(0.01-0.85)
PM _{2.5} (µg m ⁻³)	60.7	25.4	27.3	36.9	37.5(11.7-85.6)	64.5	31.4	20.7	35.1	37.6(10.1-131)	102	39.5	26.0	32.9	41.9(14.7-125)	78.1	24.2	24.6	36.8	31.2(7.74-78.9)	51.8	27.1	17.4	43.9	30.5(9.46-83.3)
3-Hydroxyglutaric acid	21.5	18.0	35.9	20.1	23.8(3.32-89.5)	18.5	13.4	19.9	32.7	20.9(2.77-54.0)	36.5	17.6	27.6	20.2	23.2(3.73-73.6)	28.0	7.80	11.0	9.26	10.5(0.62-27.9)	16.4	6.13	15.0	33.7	16.9(0.70-61.7)
3-Hydroxy-4,4-dimethylglutaric acid	10.6	12.3	24.2	15.5	15.6(1.51-57.4)	8.09	8.39	14.8	24.4	13.7(nd-35.8)	19.3	12.8	23.9	18.1	18.0(1.17-60.5)	12.6	6.39	10.4	5.60	7.93(0.27-28.5)	14.8	6.22	12.7	30.5	15.1(0.56-53.4)
cis-Pinonic acid	5.04	3.76	2.77	4.37	3.98(0.30-10.5)	6.11	5.67	2.19	6.77	4.99(0.36-20.3)	1.65	3.26	0.39	1.66	1.84(nd-11.8)	0.57	3.48	0.97	1.54	1.85(0.06-12.8)	0.37	3.01	0.83	2.02	1.62(0.14-10.3)
Pinic acid	1.40	1.03	1.40	2.33	1.54(0.10-5.10)	0.99	0.76	0.57	1.48	0.92(0.11-3.47)	0.87	0.94	0.46	0.76	0.75(0.12-2.73)	0.51	0.77	0.52	0.71	0.65(0.05-2.69)	0.37	0.31	0.52	0.63	0.45(nd-1.82)
3-Methyl-1,2,3-butanetricarboxylic acid	6.65	4.43	17.8	8.47	9.32(0.90-55.5)	7.70	5.69	10.0	14.5	9.44(0.55-25.3)	6.67	3.05	7.96	10.3	6.99(0.17-23.5)	6.76	2.34	6.90	6.80	5.52(0.07-21.0)	2.87	1.42	5.44	15.4	6.11(0.17-35.5)
Sum of SOA _M tracers	45.1	39.4	82.0	50.8	54.3(10.0-205)	41.4	33.9	47.4	79.9	50.0(9.79-118)	65.0	37.7	60.3	51.0	50.9(8.57-156)	48.5	20.8	29.8	23.9	26.5(3.24-67.3)	34.7	17.1	34.5	82.3	40.3(1.89-153)
cis-3-Methyltetrahydrofuran-3,4-diol	0.02	0.03	0.13	0.09	0.06(nd-0.40)	0.02	0.04	0.06	0.10	0.06(nd-0.14)	0.02	0.02	0.04	0.09	0.04(nd-0.26)	nd	nd	0.07	0.11	0.09(0.02-0.14)	nd	0.01	0.02	0.03	0.01(nd-0.05)
trans-3-Methyltetrahydrofuran-3,4-diol	0.04	0.08	0.64	0.25	0.25(nd-2.06)	0.04	0.05	0.16	0.21	0.12(nd-0.39)	0.05	0.04	0.10	0.22	0.11(nd-0.67)	nd	nd	0.13	0.31	0.21(0.01-0.67)	0.01	0.02	0.06	0.08	0.04(nd-0.18)
cis-2-Methyl-1,3,4-trihydroxy-1-butene	0.59	1.63	11.3	6.26	4.93(0.11-33.2)	0.39	0.85	3.32	4.50	2.27(0.02-10.6)	0.49	0.28	0.76	0.37	0.45(0.02-1.54)	0.43	0.23	1.72	2.50	1.37(0.05-5.25)	0.12	0.26	1.36	1.85	0.95(0.04-4.24)
3-Methyl-2,3,4-trihydroxy-1-butene	0.21	0.82	5.82	3.19	2.50(0.07-17.0)	0.24	0.46	1.85	2.49	1.26(0.01-5.85)	0.20	0.21	0.68	0.70	0.46(0.01-2.52)	0.33	0.12	1.01	1.65	0.85(nd-3.19)	0.05	0.13	0.75	0.89	0.49(0.01-2.31)
trans-2-Methyl-1,3,4-trihydroxy-1-butene	1.62	4.71	25.9	13.5	11.4(0.17-80.4)	0.95	1.86	7.49	11.5	5.43(0.11-29.2)	1.21	0.58	1.59	1.06	1.06(0.01-3.90)	1.24	0.64	3.46	5.11	2.85(0.09-11.3)	0.24	0.53	2.27	3.91	1.81(0.02-9.74)
2-Methylglyceric acid	2.02	3.31	3.00	3.84	3.04(0.24-9.02)	1.32	1.04	0.79	4.02	1.70(0.09-10.3)	1.56	1.41	0.94	3.09	1.83(0.07-7.75)	1.25	0.73	1.33	2.30	1.43(0.09-7.43)	0.47	0.37	0.78	1.26	0.71(0.09-3.11)
2-Methylthreitol	1.36	7.08	16.7	6.56	7.93(0.68-33.9)	0.91	1.65	4.92	5.23	3.22(0.20-15.0)	1.45	2.08	3.16	6.34	3.60(0.22-17.3)	0.97	0.54	4.08	4.17	2.88(0.11-11.9)	0.20	0.82	3.38	2.48	1.93(0.09-12.0)
2-Methylerythritol	3.31	15.5	42.4	15.5	19.1(1.59-74.7)	1.94	3.87	15.7	11.6	8.58(0.41-49.3)	2.97	4.56	8.67	14.7	8.56(0.48-42.6)	1.77	1.23	12.5	9.83	7.77(0.27-37.6)	0.44	1.86	9.49	4.69	4.79(0.25-33.9)
Sum of SOA _I tracers	9.18	33.1	106	49.2	49.3(4.86-250)	5.80	9.77	34.2	39.6	22.6(0.95-97.9)	7.95	9.18	15.9	26.2	16.0(0.95-68.6)	6.00	3.49	24.2	24.0	17.0(0.83-69.9)	1.53	3.99	18.1	15.2	10.8(0.54-62.2)
β-Caryophyllenic acid	9.76	3.70	4.02	3.40	5.22(0.40-14.3)	11.4	4.33	4.75	7.78	7.07(nd-20.5)	9.05	2.32	2.35	2.22	3.13(0.07-10.8)	8.40	1.81	1.20	1.47	1.88(0.20-8.40)	3.69	0.67	1.03	3.05	1.82(nd-5.53)
SOA _M (µg m ⁻³)	1.02	0.90	1.86	1.15	1.23(0.22-4.65)	0.94	0.77	1.08	1.81	1.13(0.22-2.69)	1.48	0.86	1.37	1.16	1.15(0.19-3.55)	1.10	0.47	0.68	0.54	0.60(0.07-1.52)	0.79	0.39	0.78	1.87	0.91(0.04-3.48)
SOA _I (µg m ⁻³)	0.11	0.41	0.99	0.41	0.47(0.05-1.85)	0.07	0.10	0.34	0.33	0.21(0.01-1.04)	0.09	0.13	0.20	0.38	0.22(0.01-1.07)	0.06	0.04	0.28	0.26	0.19(0.01-0.83)	0.02	0.05	0.22	0.13	0.11(0.01-0.76)
SOA _C (µg m ⁻³)	0.90	0.34	0.37	0.31	0.47(0.03-1.31)	1.05	0.40	0.44	0.71	0.64(nd-1.88)	0.83	0.21	0.22	0.20	0.28(0.01-0.99)	0.77	0.17	0.11	0.14	0.17(0.01-0.77)	0.34	0.06	0.09	0.28	0.16(nd-0.50)
BSOA (µg m ⁻³)	2.03	1.65	3.22	1.88	2.19(0.45-7.40)	2.06	1.27	1.85	2.86	1.99(0.45-4.21)	2.40	1.20	1.79	1.75	1.66(0.26-4.47)	1.93	0.68	1.07	0.94	0.96(0.12-2.24)	1.14	0.50	1.09	2.28	1.20(0.08-4.25)

“na” means not available and “nd” means not detected.

Table S1 Data summary of gaseous and particulate species in the air of PRD (continued)

	Tianhu (TH, rural site)					Boluo (BL, rural site)					Heshan (HS, rural site)					Taishan (TS, rural site)					9 sites average				
	Winter	Spring	Summer	Fall	Annual	Winter	Spring	Summer	Fall	Annual	Winter	Spring	Summer	Fall	Annual	Winter	Spring	Summer	Fall	Annual	Winter	Spring	Summer	Fall	Annual
Temperature (°C)	13.2	19.9	27.0	24.4	20.5(11.0-29.4)	16.4	20.5	28.6	23.4	22.7(13.9-31.4)	13.1	21.8	29.0	23.1	21.4(10.5-31.0)	16.4	23.0	29.1	23.4	22.9(14.0-31.1)	16.0	22.1	29.1	24.5	23.2(10.5-32.0)
RH (%)	na	na	na	na	na	75	75	70	71	72(60-85)	58	64	70	63	63(39-86)	75	76	71	75	74(54-84)	58	60	61	58	59(26-86)
SO ₂ (µg m ⁻³)	11.9	9.75	8.70	13.5	10.5(5.34-16.9)	15.1	10.1	10.6	15.6	13.0(5.13-20.3)	31.3	23.2	11.7	29.5	24.4(5.60-46.8)	11.6	4.35	5.46	7.15	7.14(0.95-17.0)	19.4	14.2	10.2	17.5	14.9(7.14-25.5)
NO ₂ (µg m ⁻³)	10.6	8.54	10.8	3.37	8.98(2.95-16.2)	14.1	17.6	11.4	10.7	12.9(3.78-21.4)	45.7	26.7	5.85	43.4	31.4(3.68-60.2)	38.7	14.3	13.9	18.5	21.3(6.47-49.4)	46.7	24.9	16.8	32.0	28.5(8.98-57.2)
NO (µg m ⁻³)	0.25	0.32	1.72	0.70	0.87(0.13-2.47)	1.47	1.30	0.75	0.83	1.03(0.27-2.82)	3.49	3.77	1.40	3.67	3.15(0.68-12.4)	3.58	0.47	0.63	1.13	1.45(0.08-5.78)	11.2	2.60	2.51	3.46	5.03(0.87-12.7)
NO _x (µg m ⁻³)	11.8	9.82	14.2	5.08	10.8(4.68-19.8)	17.2	20.4	14.7	12.8	15.7(8.65-26.6)	51.6	33.0	17.37	48.7	38.5(9.72-72.4)	44.0	16.1	15.8	19.8	23.9(8.08-57.0)	63.8	30.0	22.4	38.5	39.0(10.8-76.8)
O ₃ (µg m ⁻³)	99.2	84.6	90.2	139	97.2(52.8-150)	29.6	38.0	69.8	55.8	50.6(18.2-97.3)	48.7	75.4	61.0	60.4	61.3(12.8-135)	32.9	65.6	77.4	87.9	65.9(10.9-147)	52.8	64.1	73.2	79.6	67.7(50.6-97.2)
O ₂ (µg m ⁻³)	110	93.2	101	143	106(69.0-154)	43.7	55.6	81.2	66.5	63.5(27.8-112)	94.4	102	66.9	104	92.8(33.3-184)	71.6	80.0	91.2	106	87.2(25.8-173)	99.5	88.9	90.0	112	96.1(63.5-112)
CO (mg m ⁻³)	0.62	0.57	0.56	0.32	0.54(0.26-0.87)	0.85	0.67	0.51	0.54	0.62(0.30-1.06)	1.10	0.88	0.87	0.82	0.91(0.50-1.22)	0.88	0.56	0.54	0.78	0.68(0.30-1.04)	1.00	0.73	0.65	0.65	0.74(0.54-0.94)
OC (µgC m ⁻³)	8.05	5.38	6.30	8.05	6.49(3.64-10.4)	7.40	6.63	7.03	8.67	7.52(2.64-16.7)	12.9	6.82	6.31	12.6	9.65(2.74-22.4)	10.8	6.79	8.28	12.8	9.67(4.24-23.1)	13.7	6.30	6.53	8.74	8.50(1.93-33.4)
EC (µgC m ⁻³)	1.44	0.96	1.04	na	1.13(0.40-2.04)	2.98	1.99	1.92	2.08	2.22(0.54-8.22)	3.38	1.86	1.36	3.51	2.52(0.52-6.19)	3.22	1.28	1.66	3.14	2.32(0.64-6.86)	4.00	1.47	1.55	2.47	2.23(0.40-11.6)
SO ₄ ²⁻ (µg m ⁻³)	9.83	6.32	5.11	na	7.18(2.99-15.1)	4.38	10.11	6.40	5.97	6.45(2.10-18.5)	10.4	6.96	5.43	13.9	9.17(2.24-28.2)	11.3	5.98	7.09	13.3	9.41(2.12-18.9)	11.8	7.28	6.32	9.31	8.44(2.10-28.2)
NO ₃ ⁻ (µg m ⁻³)	1.00	1.27	0.09	na	0.88(0.01-2.93)	2.69	3.50	0.48	0.60	1.56(0.11-8.66)	8.33	3.01	0.30	5.32	4.23(0.15-16.3)	9.49	2.23	0.40	2.81	3.73(0.12-23.7)	8.12	2.41	0.42	1.64	2.65(0.01-23.7)
NH ₄ ⁺ (µg m ⁻³)	3.80	2.52	1.94	na	2.80(1.11-5.88)	2.43	4.58	2.42	2.38	2.79(0.77-8.96)	5.92	3.50	2.14	6.06	4.40(0.85-13.8)	6.32	3.01	2.57	5.22	4.28(0.44-11.3)	6.66	3.34	2.41	3.63	3.74(0.44-14.2)
Cl ⁻ (µg m ⁻³)	0.05	0.07	0.02	na	0.04(nd-0.15)	0.54	0.40	0.05	0.08	0.23(0.01-1.77)	1.20	0.46	0.05	0.32	0.50(0.01-1.85)	1.54	0.26	0.06	0.24	0.52(0.01-4.20)	1.00	0.33	0.07	0.14	0.33(nd-4.20)
Na ⁺ (µg m ⁻³)	0.57	0.48	0.14	na	0.42(0.04-0.75)	0.10	0.26	0.43	0.25	0.27(0.03-1.00)	0.71	0.31	0.24	0.59	0.46(0.18-1.29)	0.49	0.28	0.35	0.70	0.45(0.18-0.96)	0.57	0.47	0.31	0.38	0.44(0.03-2.66)
K ⁺ (µg m ⁻³)	0.43	0.24	0.12	na	0.27(0.06-0.57)	0.27	0.24	0.19	0.20	0.22(0.07-0.71)	1.02	0.35	0.32	0.81	0.62(0.11-1.50)	0.49	0.16	0.42	0.52	0.39(0.09-1.02)	0.72	0.27	0.21	0.34	0.36(0.01-2.16)
Mg ²⁺ (µg m ⁻³)	0.08	0.07	0.02	na	0.05(nd-0.10)	0.02	0.03	0.03	0.04	0.03(0.01-0.07)	0.04	0.03	0.02	0.04	0.03(nd-0.09)	0.02	0.03	0.03	0.04	0.02(nd-0.06)	0.06	0.06	0.04	0.04	0.05(nd-0.34)
Ca ²⁺ (µg m ⁻³)	0.46	0.42	0.10	na	0.35(0.04-0.85)	0.18	0.16	0.25	0.34	0.24(0.10-0.62)	0.34	0.13	0.13	0.36	0.24(0.02-0.66)	0.20	0.19	0.19	0.31	0.22(0.12-0.40)	0.36	0.29	0.23	0.29	0.30(nd-1.14)
PM _{2.5} (µg m ⁻³)	33.9	21.6	18.9	na	25.0(9.98-43.0)	31.4	30.5	24.5	28.7	28.4(11.0-72.5)	63.1	29.8	21.4	54.9	42.2(6.78-112)	55.3	21.1	24.5	52.6	38.3(7.68-114)	60.1	27.8	22.8	35.7	34.7(6.78-131)
3-Hydroxyglutaric acid	21.0	18.1	22.0	35.6	22.2(4.44-52.4)	14.1	16.4	24.3	16.5	18.1(3.64-74.8)	16.3	14.7	24.0	35.7	22.6(2.72-89.4)	19.0	5.25	23.4	42.0	22.4(1.44-79.2)	21.2	13.1	22.6	27.3	20.1(10.5-23.8)
3-Hydroxy-4,4-dimethylglutaric acid	10.7	15.2	15.0	35.5	16.6(1.65-36.8)	6.20	13.9	18.4	19.1	14.9(0.77-53.6)	7.87	12.5	19.6	26.7	16.6(2.11-61.0)	7.49	4.36	15.5	25.7	13.2(nd-47.9)	10.8	10.2	17.2	22.3	14.7(7.93-18.0)
cis-Pinonic acid	11.8	6.26	4.03	29.3	10.2(0.66-34.3)	1.80	1.16	1.57	2.22	1.74(0.28-5.34)	6.81	3.32	2.01	2.41	3.63(0.56-18.5)	7.55	3.91	2.01	1.82	3.82(0.08-26.1)	4.64	3.76	1.86	5.79	3.75(1.62-10.2)
Pinic acid	1.70	0.92	1.33	6.58	1.99(0.19-7.69)	0.73	0.49	0.66	0.94	0.72(0.12-1.80)	1.17	0.65	0.77	1.45	1.01(0.14-3.17)	0.63	0.95	1.02	1.44	1.00(0.13-2.43)	0.93	0.76	0.81	1.81	1.01(0.45-1.99)
3-Methyl-1,2,3-butanetricarboxylic acid	4.48	3.76	5.37	18.3	6.31(0.75-18.8)	6.89	3.68	12.1	10.4	8.91(0.35-34.5)	3.18	7.44	14.1	9.73	8.62(0.92-18.1)	6.98	2.08	6.68	13.8	7.39(0.40-25.8)	5.80	3.76	9.60	12.0	7.63(5.52-9.44)
Sum of SOA _M tracers	49.7	44.3	47.7	125	57.4(15.5-134)	29.7	35.6	57.0	49.2	44.5(7.51-164)	35.3	38.6	60.5	76.0	52.5(12.3-167)	41.7	16.5	48.6	84.9	47.9(4.82-157)	43.5	31.6	52.0	69.2	47.1(26.5-57.4)
cis-3-Methyltetrahydrofuran-3,4-diol	0.01	0.02	0.04	0.13	0.03(nd-0.16)	0.02	0.02	0.07	0.14	0.07(nd-0.51)	0.02	0.01	0.05	0.10	0.04(nd-0.22)	0.02	0.06	0.05	0.12	0.06(nd-0.18)	0.02	0.03	0.06	0.10	0.05(0.01-0.09)
trans-3-Methyltetrahydrofuran-3,4-diol	0.02	0.04	0.08	0.33	0.08(nd-0.42)	0.03	0.04	0.22	0.35	0.18(nd-1.21)	0.03	0.03	0.24	0.30	0.15(nd-0.67)	0.04	0.13	0.13	0.25	0.13(0.01-0.48)	0.03	0.05	0.20	0.26	0.14(0.04-0.25)
cis-2-Methyl-1,3,4-trihydroxy-1-butene	0.28	0.31	1.32	7.20	1.48(0.05-8.95)	0.19	0.10	1.77	1.55	1.00(0.01-5.64)	0.31	0.27	1.66	2.91	1.28(0.04-7.09)	0.24	0.12	2.01	5.88	2.19(0.03-12.0)	0.34	0.45	2.80	3.67	1.77(0.45-4.93)
3-Methyl-2,3,4-trihydroxy-1-butene	0.17	0.19	0.89	5.49	1.07(nd-6.86)	0.13	0.08	1.41	1.18	0.78(nd-4.53)	0.16	0.22	1.53	2.38	1.07(nd-5.23)	0.14	0.04	1.06	2.82	1.15(nd-5.94)	0.18	0.25	1.67	2.31	1.07(0.46-2.50)
trans-2-Methyl-1,3,4-trihydroxy-1-butene	0.67	0.71	2.98	15.6	3.29(0.13-17.8)	0.44	0.30	3.70	3.17	2.11(0.04-12.3)	0.77	0.71	3.70	7.29	3.11(0.10-17.1)	0.56	0.16	4.28	13.3	5.21(0.05-30.3)	0.86	1.13	6.15	8.28	4.03(1.06-11.4)
2-Methylglyceric acid	1.43	1.03	1.23	4.80	1.68(0.31-5.54)	0.77	0.69	1.89	4.78	2.26(0.23-13.5)	1.50	1.23	2.27	5.87	2.71(0.10-10.8)	1.15	1.48	2.44	5.10	2.54(0.15-13.7)	1.28	1.25	1.63	3.90	1.99(0.71-3.04)
2-Methylglythreitol	0.98	1.76	6.12	18.8	4.98(0.26-25.6)	1.12	1.60	7.80	6.91	4.87(0.34-17.1)	0.87	1.22	7.25	6.91	4.06(0.25-12.9)	1.10	1.33	5.93	7.78	4.03(0.26-15.4)	1.00	2.01	6.60	7.24	4.17(1.93-7.93)
2-Methylethritol	1.85	3.46	14.2	37.2	10.4(0.36-49.2)	2.44	3.05	19.9	15.8	11.6(0.75-48.9)	2.07	2.62	19.4	14.1	9.54(0.70-30.0)	2.44	2.81	18.0	16.0	9.79(0.59-31.8)	2.14	4.32	17.8	15.5	10.0(4.79-19.1)
Sum of SOA _I tracers	5.41	7.50	26.9	89.6	23.0(1.45-113)	5.13	5.87	36.7	32.7	22.6(1.54-93.8)	5.74	6.30	36.1	39.8	21.9(1.38-77.3)	5.68	5.95	33.9	51.2	24.1(1.19-103.)	5.82	9.46	36.9	40.8	23.0(10.8-49.3)
β-Caryophyllenic acid	9.17	3.84	2.96	5.17	5.20(1.77-11.8)	3.71	2.33	2.33	2.30	2.64(0.45-8.47)	6.73	2.38	2.99	5.17	4.31(1.45-10.3)	5.49	0.11	2.88	4.79	3.31(nd-11.4)	7.49	2.39	2.73	3.93	3.84(1.82-7.07)
SOA _M (µg m ⁻³)	1.13	1.01	1.08	2.84	1.30(0.35-3.05)	0.67	0.81	1.29	1.12	1.01(0.17-3.73)	0.80	0.88	1.37	1.72	1.19(0.28-3.79)	0.95	0.38	1.10	1.93	1.08(0.10-3.56)	0.99	0.72	1.18	1.57	1.07(0.60-1.30)
SOA _I (µg m ⁻³)	0.07	0.10	0.34	0.97	0.27(0.01-1.25)	0.07	0.08	0.47	0.44	0.29(0.02-1.11)	0.07	0.08	0.46	0.43	0.25(0.01-0.82)	0.07	0.09	0.42	0.46	0.25(0.01-0.85)	0.07	0.12	0.41	0.42	0.25(0.11-0.47)
SOA _C (µg m ⁻³)	0.84	0.35	0.27	0.47	0.47(0.16-1.08)	0.34	0.21	0.21	0.21	0.24(0.04-0.77)	0.62	0.22	0.27	0.47	0.39(0.13-0.94)	0.50	0.01	0.26	0.44	0.30(nd-1.05)	0.69	0.22	0.25	0.36	0.35(0.16-0.64)
BSOA (µg m ⁻³)	2.04	1.46	1.70	4.28	2.05(0.53-4.33)	1.08	1.11	1.98	1.76	1.55(0.26-5.35)	1.49	1.18	2.11	2.62	1.84(0.56-5.43)	1.52	0.47	1.79	2.82	1.65(0.16-5.24)	1.74	1.06	1.84	2.35	1.68(0.96-2.19)

“na” means not available and “nd” means not detected.

Table S2 SOA tracers and f_{SOA} and f_{SOC} values for SOA estimation

	Monoterpenes ^a	Isoprene ^b	β -Caryophyllene ^b
SOA Tracers ^c	PNA (15%) ^d PA (34%) ^d MBTCA (62%) ^d HGA (96%) ^d HDMGA (67%) ^d	2-MTLs (41%) ^d 2-MGA (43%) ^d 3-MeTHF-3,4-diols (52%) C ₅ -alken triols (93%)	CA (157%) ^d
f_{SOA} ($\mu\text{g } \mu\text{g}^{-1}$)	0.044 (48%) ^e	0.063 (25%) ^e	0.0109 (22%) ^e
f_{SOC} ($\mu\text{g } \mu\text{gC}^{-1}$)	0.059	0.155	0.023

^a The f_{SOA} and f_{SOC} values for monoterpenes are calculated based on the data reported by Offenberger et al. (2007). ^b The f_{SOA} and f_{SOC} values for isoprene, and β -caryophyllene are reported by Kleindienst et al. (2007). ^c The numbers in brackets are uncertainties in tracer measurement. ^d These tracers are used to calculate f_{SOA} and estimate ambient SOA. ^e The numbers in brackets are the uncertainties of f_{SOA} values reported by Kleindienst et al. (2007).

Table S3 Correlation analysis of HO₂-channel SOA_I tracers with O₃

	Coefficient (r)	<i>p</i> -value
3-MeTHF-3,4-diols	0.343	<0.001
C ₅ -alkene triols	0.388	<0.001
2-Methyltetrols	0.386	<0.001
HO ₂ -channel SOA _I tracers	0.409	<0.001

Table S4 Correlations among HO₂-channel SOA_I tracers

	3-MeTHF-3,4-diols	C ₅ -alkene triols	2-Methyltetrols
3-MeTHF-3,4-diols	1	0.789	0.792
C ₅ -alkene triols		1	0.787
2-Methyltetrols			1

All the correlations are significant ($p < 0.001$)

Table S5 Rate constants and lifetimes of SOA precursors

	α -Pinene	β -Pinene	Isoprene	β -Caryophyllene
Rate constants at 298 K ($\text{cm}^3 \text{ molecules}^{-1} \text{ s}^{-1}$) ^a				
OH	5.25×10^{-11}	7.88×10^{-11}	9.99×10^{-11}	1.97×10^{-10}
O ₃	9.01×10^{-17}	1.50×10^{-17}	1.28×10^{-17}	1.16×10^{-14}
Lifetimes (hrs) ^b				
OH	0.53	0.35	0.28	0.14
O ₃	3.64	21.9	25.7	0.03

^a Rate constants are provided by MCMv3.2 (<http://mcm.leeds.ac.uk/MCMv3.2>).

^b Lifetimes are estimated using summer average concentration of OH radical ($\sim 1 \times 10^7 \text{ molecules cm}^{-3}$) in the PRD (Hofzumahaus et al., 2009), and annual average O₃ concentration ($67.7 \mu\text{g m}^{-3}$) in Table S1.

Table S6 Concentrations of isoprene SOA products at HS and TS sites

	HS 20150701	TS 20150701
2-Methyltetrol sulfates (ng m^{-3})	6.65	2.99
C ₅ -alkene triols (ng m^{-3})	11.5	10.8
2-Methyltetrols (ng m^{-3})	41.8	31.2
3-MeTHF-3,4-diols (ng m^{-3})	0.482	0.227

Table S7 Correlations of BSOA with sulfate and O₃ during fall-winter in 2008 at WQS

	Sulfate (2008-WQS)			O ₃ (2008-WQS)	
	Slope	<i>p</i> -value	% ^a	Slope	<i>p</i> -value
SOA _M	0.023	0.005	50	-	0.551
SOA _I	0.032	<0.001	76	-	0.509
SOA _C	0.032	<0.001	87	-	0.139
BSOA	0.087	<0.001	69	-	0.563

^a Percentages of SOA reduction at 50% decline of sulfate or O₃.**References:**

- Ding, X., Wang, X., Gao, B., Fu, X., He, Q., Zhao, X., Yu, J., and Zheng, M.: Tracer based estimation of secondary organic carbon in the Pearl River Delta, South China, *J. Geophys. Res-Atmos.*, 117, D05313, 10.1029/2011JD016596, 2012.
- Ding, X., He, Q. F., Shen, R. Q., Yu, Q. Q., and Wang, X. M.: Spatial distributions of secondary organic aerosols from isoprene, monoterpenes, β -caryophyllene, and aromatics over China during summer, *J. Geophys. Res-Atmos.*, 119, 11877-11891, 10.1002/2014JD021748, 2014.
- Ding, X., Zhang, Y. Q., He, Q. F., Yu, Q. Q., Shen, R. Q., Zhang, Y., Zhang, Z., Lyu, S. J., Hu, Q. H., Wang, Y. S., Li, L. F., Song, W., and Wang, X. M.: Spatial and seasonal variations of secondary organic aerosol from terpenoids over China, *J. Geophys. Res-Atmos.*, 121, 14661-14678, 10.1002/2016JD025467, 2016.
- Eddingsaas, N. C., Loza, C. L., Yee, L. D., Chan, M., Schilling, K. A., Chhabra, P. S., Seinfeld, J. H., and Wennberg, P. O.: α -pinene photooxidation under controlled chemical conditions – Part 2: SOA yield and composition in low- and high-NO_x environments, *Atmos. Chem. Phys.*, 12, 7413-7427, 10.5194/acp-12-7413-2012, 2012.
- Hofzumahaus, A., Rohrer, F., Lu, K., Bohn, B., Brauers, T., Chang, C.-C., Fuchs, H., Holland, F., Kita, K., Kondo, Y., Li, X., Lou, S., Shao, M., Zeng, L., Wahner, A., and Zhang, Y.: Amplified trace gas removal in the troposphere, *Science*, 324, 1702-1704, 10.1126/science.1164566, 2009.
- Hu, D., Bian, Q., Li, T. W. Y., Lau, A. K. H., and Yu, J. Z.: Contributions of isoprene, monoterpenes, β -caryophyllene, and toluene to secondary organic aerosols in Hong Kong during the summer of 2006, *J. Geophys. Res-Atmos.*, 113, D22206, 10.1029/2008JD010437, 2008.
- Kleindienst, T. E., Jaoui, M., Lewandowski, M., Offenberg, J. H., Lewis, C. W., Bhawe, P. V., and Edney, E. O.: Estimates of the contributions of biogenic and anthropogenic hydrocarbons to secondary organic aerosol at a southeastern US location, *Atmos. Environ.*, 41, 8288-8300, 10.1016/j.atmosenv.2007.06.045, 2007.
- Lewandowski, M., Piletic, I. R., Kleindienst, T. E., Offenberg, J. H., Beaver, M. R., Jaoui, M., Docherty, K. S., and Edney, E. O.: Secondary organic aerosol characterisation at field sites across the United States during the spring-summer period, *Int. J. Environ. An. Ch.*, 93, 1084-1103, 10.1080/03067319.2013.803545, 2013.
- Lin, Y.-H., Zhang, Z., Docherty, K. S., Zhang, H., Budisulistiorini, S. H., Rubitschun, C. L., Shaw, S., Knipping, E., Edgerton, E. S., Kleindienst, T. E., Gold, A., and Surratt, J. D.: Isoprene epoxydiols as

删除的内容: .

分页符

带格式的: 字体: 小四

precursors to secondary organic aerosol formation: Acid-catalyzed reactive uptake studies with authentic standards, Environ. Sci. Technol., 46, 189-195, 10.1021/es202554c, 2012.

Offenberg, J. H., Lewis, C. W., Lewandowski, M., Jaoui, M., Kleindienst, T. E., and Edney, E. O.: Contributions of toluene and α -pinene to SOA formed in an irradiated toluene/ α -pinene/ NO_x /air mixture: Comparison of results using ^{14}C content and SOA organic tracer methods, Environ.Sci. Technol., 41, 3972-3976, 10.1021/es070089+, 2007.

Riva, M., Budisulistiorini, S. H., Zhang, Z., Gold, A., and Surratt, J. D.: Chemical characterization of secondary organic aerosol constituents from isoprene ozonolysis in the presence of acidic aerosol, Atmos. Environ., 130, 5-13, 10.1016/j.atmosenv.2015.06.027, 2016.

Stone, E. A., Nguyen, T. T., Pradhan, B. B., and Man Dangol, P.: Assessment of biogenic secondary organic aerosol in the Himalayas, Environ. Chem., 9, 263-272, 10.1071/EN12002, 2012.

Von Schneidmesser, E., Zhou, J., Stone, E. A., Schauer, J. J., Shpund, J., Brenner, S., Qasrawi, R., Abdeen, Z., and Sarnat, J. A.: Spatial variability of carbonaceous aerosol concentrations in east and west Jerusalem, Environ. Sci. Technol., 44, 1911-1917, 10.1021/es9014025, 2009.

Zheng, J., Zheng, Z., Yu, Y., and Zhong, L.: Temporal, spatial characteristics and uncertainty of biogenic VOC emissions in the Pearl River Delta region, China, Atmos. Environ., 44, 1960-1969, 10.1016/j.atmosenv.2010.03.001, 2010.

删除的内容:

带格式的: 缩进: 左侧: 0 厘米, 悬挂缩进: 1 字符, 首行缩进: -1 字符, 行距: 1.5 倍行距

删除的内容: 。

。